Received: 22 January 2021 | Revised: 14 September 2021 | Accepted: 14 September 2021

DOI: 10.1002/fut.22273

RESEARCH ARTICLE

THE JOURNAL OF FUTURES MARKETS WILEY

A Skellam market model for *loan prime rate* options

Zhanyu Chen[1] | **Kai Zhang**[2] | **Hongbiao Zhao**[3,4]

[1]Shanghai Clearing House, Shanghai, China

[2]J.P. Morgan, London, UK

[3]School of Statistics and Management, Shanghai University of Finance and Economics, Shanghai, China

[4]Shanghai Institute of International Finance and Economics, Shanghai, China

Correspondence
Hongbiao Zhao, School of Statistics and Management, Shanghai University of Finance and Economics, No. 777 Guoding Rd, 200433 Shanghai, China.
Email: h.zhao1@lse.ac.uk

Funding information
National Natural Science Foundation of China, Grant/Award Number: 71401147; Shanghai University of Finance and Economics, Grant/Award Number: 2020110930

Abstract

This paper documents vanilla interest-rate options newly introduced in China. The underlying rates are the RMB loan prime rates (LPRs), the foremost interest rates that matter to almost all businesses and households in China. They are digital with a tick size of five basis points, and the changes only occur monthly at predetermined announcement times. We propose a novel continuous-time discrete-state market model based on the integer-valued Skellam distribution, and derive arbitrage-free pricing formulas in closed forms. We advocate that it is more meaningful to quote LPR option prices in terms of implied intensity rather than implied volatility.

KEYWORDS
implied intensity, intensity smile, loan prime rate (LPR), loan prime rate option, prescheduled macroeconomic announcements, Skellam market model

JEL CLASSIFICATION
G13, G12, C51, E43

1 | INTRODUCTION

On 23 March 2020, China started trading vanilla interest-rate options including caps, floors, and swaptions, which protect lenders and borrowers against interest rate fluctuations, in interbank markets via the platform of the National Interbank Funding Center (NIFC). The aim is to enable the China's interbank interest-rate derivatives market to play a better role in supporting the real economy, to meet investors' interest rate risk management demands and improve the market-led interest-rate pricing mechanism. This adds a new milestone to the government's efforts to liberalize interest rates in China. With the domestic bonds outstanding of CNY 84.2 trillion (USD 12.1 trillion) at the end of December 2019 estimated by Asian Development Bank,[1] demands for interest-rate options would be potentially tremendous.

The underlying of these options is the RMB *loan prime rate* (LPR), the foremost interest rate that matters to businesses and households in China. The LPR is the lending rate provided by commercial banks to their highest-quality customers and prime clients, and it serves as the benchmark for lending rates provided for other loans by adding or subtracting basis points based on it. For example, the 1-year tenor LPR serves as the baseline for domestic corporate borrowing with debt outstanding amount of about CNY 30 trillions (USD 4.3 trillion), and the 5-year tenor LPR serves as a baseline for housing mortgage loans of about CNY 30 trillions (USD 4.3 trillion).[2] The current LPR quotation group is comprised of 18 commercial banks in China, including an original core group of ten national banks, two municipal

[1]For more overview data on China's bond market, see https://asianbondsonline.adb.org.
[2]For more details on the current Chinese bond market and interbank market, see Schipke et al. (2019) and Amstad and He (2020).

commercial banks, two rural village commercial banks, two foreign invested banks, and two privately operated banks. China's central bank, the People's Bank of China (PBOC), has authorized the NIFC to serve as the designated publisher of the LPR.

Since the LPR reformed on August 20, 2019, the LPR is called "new LPR" as rates shift toward market-led system, similar as the system for the London Interbank Offered Rate (LIBOR) (Duffie & Stein, 2015). The panel banks submit quotations to the NIFC, with 0.05% or 5 basis points (bps) as *tick size*, before 9:00 a.m. (GMT+8) on the 20th day of each month (holidays postpone). Quotations are partially determined by referring the *medium-term lending facility*, a liquidity policy toolkit created in 2014 by the PBOC for longer-term loans. So, the LPR can be considered as a hybrid rate shaped by China's central bank and major commercial banks. The NIFC calculates the arithmetic average of quotations, after removing the highest and lowest quotes, and approximates to integral multiple times of 5 bps to conclude the final LPR. At 9:30 a.m. (GMT+8), the LPR is released to the general public at websites of NIFC and PBOC. Currently, the 1-year LPR (*1Y LPR*) and the 5-year LPR (*5Y LPR*) are published since August 20, 2019, and they are released monthly.[3] Since August 20, 2019, the LPR changes monthly on predetermined dates as a step function of multiples of 5 bps. The daily time series of spot 1Y LPR and 5Y LPR are plotted in Figure 1. It is *digital* with a tick size of 5 bps and changes only occur at predetermined times. Interestingly, as we can see from Figure 1, there are some unique stylized features of the randomness in LPR time series: (1) nonnormal distribution for underlying returns; (2) pure-jump process (without diffusion); (3) deterministic jump timing on the 20th day of each month (holidays postpone); (4) discrete-state jump sizes, that is, since August 20, 2019, the LPR changes can only be the multiples of 5 bps. Note that, it is similar to but different from the well known US *federal funds rate target*. This rate is also a pure-jump process with 25-bp tick-size movements, but there still exists some uncertainty in the *timing* of jumps: its *jump intensity* depends not only on the scheduled meeting calendar of the Federal Open Market Committee (FOMC) but also on the macro state of the economy, see for example, Clarida et al. (2000), Piazzesi (2001, 2005, 2010), Cochrane and Piazzesi (2002), and Hamilton and Jordà (2002). Potentially, China's LPR might offers the purest environment in the real world for investigating the impacts of *prescheduled* macroeconomic events to asset prices. Our primary aim of this paper is to provide a simplest extension of the standard Black model for interest-rate option pricing that parsimoniously accommodates these key stylized features in Figure 1 and this could also offer the foundation for more comprehensive and realistic models in the future.

As early pointed out by Bates (1996, p. 567), the central empirical issue in option research is whether the distributions implicit in option prices are consistent with the time series properties of the underlying asset prices. In this paper, we aim to develop a concise model for pricing vanilla LPR options, which is consistent with these stylized features as presented in Figure 1. Our model can be considered as an extension of the classical LIBOR market model, which is mainly developed by Miltersen et al. (1997), Brace et al. (1997) and Jamshidian (1997) further upon the HJM framework of Heath et al. (1992) for instantaneous forward rates. Andersen and Andreasen (2000) and Joshi and Rebonato (2003) extended it to local volatility models based on constant elasticity of variance (CEV) process and displaced-diffusion process, respectively. Andersen and Brotherton-Ratcliffe (2001) and Han (2007) introduced stochastic volatility models based on the CIR process (Cox et al., 1985), and Hagan et al. (2002) developed the SABR model which is now widely used in industry. Moreover, Glasserman and Kou (2003) and R. Jarrow et al. (2007) extended to jump-diffusion models, and Eberlein and Özkan (2005), and Leippold and Strømberg (2014) advanced to Lévy processes.

Although the current literature on interest-rate option pricing is voluminous, these unique features presented in Figure 1 bring a new challenge, as most models are based on diffusion processes or jump processes with random jump timing (e.g., Lévy-driven processes[4]). Instead, the key ingredient in our new model is the integer-valued Skellam distribution early introduced by Skellam (1946). Skellam distribution, defined as the difference of two Poisson random variables, has been recently used and modified for modeling the goal difference of two opposing teams by Karlis and Ntzoufras (2003) and high-frequency tick-by-tick discrete price changes by Koopman et al. (2017). A few literature considered the *predetermined* jump timing (e.g. for the US Federal Open Market Committee meetings or monthly employment reports) in modeling interest rates, see for example, Piazzesi (2001, 2005, 2010) and Kim and Wright (2016). However, their models are very different from our Skellam-based continuous-time model, and they have additional diffusion components and were used primarily for analyzing time series of short-term interest rates or

[3]For more details and the historical data of spot LPR, see http://www.chinamoney.com.cn/chinese/bklpr.
[4]It is well known that, any Lévy process has no *fixed* times of discontinuity due to its path property of *stochastic continuity*, see Sato (1999).

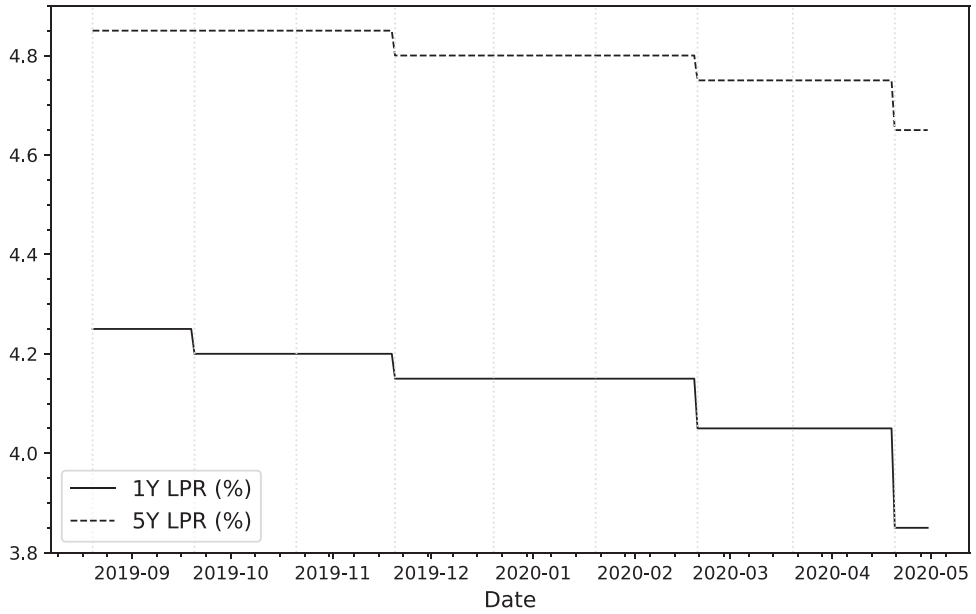

FIGURE 1 Daily time series of *spot* loan prime rates (1Y LPR and 5Y LPR, 20/8/2019–30/4/2020). LPR, loan prime rate

pricing discount bonds rather than pricing interest-rate derivatives. A very few and seemingly relevant literature, such as Carr (2011) and Barndorff-Nielsen et al. (2012), adopted Skellam *processes* for derivative pricing. However, these processes are special cases of Lévy processes with *random* jump timing which are unsuitable for modeling the LPR with *fixed* jump timing; moreover, they were applied to equity options rather than market-based interest-rate options, and the *tick-size effect* or *discreteness effect* in equity markets is generally much smaller than the one here in LPR interest-rate markets due to the change sizes relative to the underlying levels. Traditional discrete-time (finite) discrete-state lattice-based models, such as binomial trees and trinomial trees, and are of course too restrictive to model the LPR, since *marginally* the level of LPR has the possibility of moving in multiple ticks just at a single announcement day, and *horizontally* these lattice-based models fail to capture the continuous-time dynamics of LPR between any two successive announcement times.

Our main contribution of this paper is the theoretical development of a pure-jump *Skellam market model* with deterministic jump timing[5] for pricing LPR options in analytical forms, which is consistent with our observation of LPR time series with unique features as plotted in Figure 1. This consistence between the risk-neutral world and natural world is achieved by a proper change of measure which guarantees no arbitrage. It is important, as it would further facilitate more efficient risk management and more accurate option-implied forward-looking analysis. This new theoretical model is tailored and first applied to the China's interest-rate options markets, and it is potentially applicable for other markets if the underlying of traded options presents similar stylized features. Our key finding of great interest in general is that, different from traditional options, the risk-neutral *intensity* (rather than *diffusion*) plays a dominant role in pricing these new LPR derivatives, which resemble the more familiar credit derivatives. In addition, our preliminary empirical work shows that, the LPR's jump intensity, the only parameter in the model, presents *intensity frown* implied from cap prices and *intensity skew* implied from swaption prices, which call for future research of model extensions. Moreover, we derive algorithms for constructing a simple forward LPR curve from swap rate data, which would act as the infrastructure for a further development of LPR option market.

This paper is organized as follows: Section 2 introduces our benchmark model for the LPR time series and summarizes its key properties. In Section 3, we explain the LPR swap market, and develop algorithms for constructing a simple forward LPR curve from swap rate data. Section 4, the main contribution of this paper, introduces the LPR option market and develops our new market models based on the integer-valued Skellam distribution for pricing

[5]Literature on option pricing with deterministic jump timing is also very rare, see a recent work by Dubinsky et al. (2019) for pricing equity options. These jumps are used for modeling *prescheduled* earning announcements. However, they adopted a jump-diffusion model living on a continuous-state space, which is different from our pure-jump model on a discrete-state space.

vanilla interest-rate options (caps, floors, and swaptions) in closed forms. Section 5 draws a brief conclusion for this paper, and proposes some issues for further extensions and future research.

2 | BENCHMARK MODEL FOR LPR

In this section, we introduce a benchmark model for LPR time series. The aim is to keep our model as parsimonious as possible but without losing key stylized facts as observed in Figure 1. Let us first construct a *continuous-time* model for the dynamics of discrete-valued spot LPR as observed in Figure 1. The time-t*spot LPR*, for lending to borrowers for the period $[t, t+\tau]$ with a fixed period τ prevailing at time t, is denoted by $L(t, t+\tau)$. There are only two choices for τ: $\tau = 1, 5$ in the unit of year. For simplicity, we denote both by

$$L(t) \coloneqq L(t, t+\tau), t \geq 0,$$

which is characterized by the stochastic differential equation (SDE)

$$\mathrm{d}L(t) = b\mathrm{d}\mathbf{D}(t), \tag{1}$$

where

- $\mathbf{D}(t)$ is a pure-jump process on a probability space $(\Omega, \mathcal{F}, \mathbb{P})$ with a given filtration $\{\mathcal{F}_t\}_{t\geq 0}$,

$$\mathbf{D}(t) \coloneqq \sum_{k=0}^{n(t)} D(k), D(\cdot) \in \mathbb{Z},$$

- $b > 0$ is a constant representing the minimum amount that the LPR can change, that is, *tick size* ($b = 0.05\%$ here);
- $n(t)$ is a *deterministic* right-continuous[6] point process with $n(0) = 0$, as illustrated in Figure 2, counting the total number of LPR-announcement times within the period $(0, t]$, that is,

$$n(t) \coloneqq \sum_{k=1}^{\infty} \mathbf{1}\{a_k \leq t\},$$

- $\{a_k\}_{k=1, \ldots}$ are the ordered sequence of predetermined *LPR-announcement times*, and $\mathbf{1}\{\cdot\}$ is the indicator function;
- *tick change* $D(k)$ is an integer on the set of integers $\mathbb{Z} \coloneqq \{0, \pm 1, \pm 2, ...\}$, representing the number of ticks that the spot LPR changes at LPR-announcement arrival time a_k, and define $D(0) \coloneqq 0$.

Solving the SDE (1) conditional on initial level $L(0)$ gives the dynamics of LPR,

$$L(t) = L(0) + b\sum_{k=0}^{n(t)} D(k) = L(0) + b\mathbf{D}(t). \tag{2}$$

In fact, the discrete-valued random jump size at each LPR-announcement arrival time can be iteratively expressed by

$$\Delta L(a_{k+1}) \coloneqq L(a_{k+1}) - L(a_{k+1}^-) = bD(k+1), k = 1, ...,$$

where $L(a_{k+1}^-) = L(a_k)$. The integer-valued time series $\{D(k)\}_{k=1, \ldots}$ are the only random components in LPR dynamics (2). The LPR announcements occur monthly. If we ignore occasional announcement delays due to weekends or

[6] i.e., $n(t) = \lim_{s \downarrow t} n(s)$.

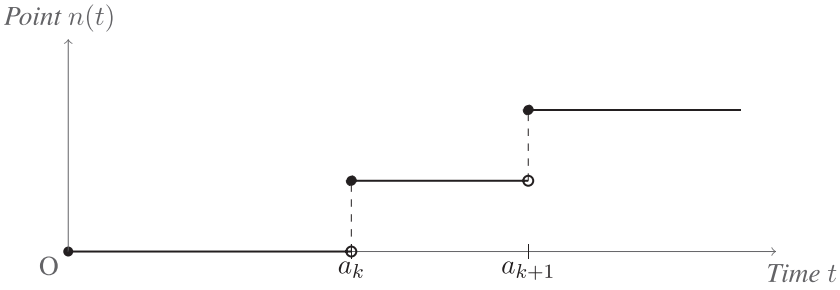

FIGURE 2 A deterministic right-continuous point process $n(t)$

holidays for simplicity, $a_{k+1} - a_k = 1/12$ for any $k = 1, \ldots$ and $a_1 \in (0, 1/12]$. So, $n(t)$ is a *deterministic* function of t which can be written explicitly in general as

$$n(t) = \lfloor 12(t - a_1) \rfloor + 1, t \geq 0,$$

where $\lfloor u \rfloor$ is the *floor* under u, that is, the greatest integer less than or equal to u. In particular, if $a_1 = 1/12$, then, it is simplified as

$$n(t) = \lfloor 12t \rfloor, t \geq 0.$$

Obviously, $n(t) - n(s) = n(t - s)$ does not hold for all $s \in [0, t)$ in general. Due to this *nonstationary* (*time-inhomogeneous*) nature of deterministic process $n(t)$, the resulting LPR process $L(t)$ cannot be modeled appropriately by most existing models (e.g. Lévy processes) in the literature.

The key ingredient in our new model is the Skellam distribution for modeling tick change $D(\cdot)$. *Skellam distribution* (Skellam, 1946) or *Poisson-difference distribution*, is an integer-valued distribution, simply constructed as the difference between two independent Poisson-distributed random variables N^+, N^- with constant *rate parameters* $\lambda^+, \lambda^- > 0$, respectively, that is,

$$D \coloneqq N^+ - N^-,$$

which is denoted as $D \sim \mathrm{SK}(\lambda^+, \lambda^-)$ on $\mathbb{Z}$. The probability mass function (PMF) of D is

$$\Pr\{D = d; \lambda^+, \lambda^-\} = e^{-(\lambda^+ + \lambda^-)} \left(\frac{\lambda^+}{\lambda^-}\right)^{\frac{d}{2}} \mathrm{I}_{|d|}(2\sqrt{\lambda^+\lambda^-}), d \in \mathbb{Z}, \tag{3}$$

where $\mathrm{I}_d(\cdot)$ is the *modified Bessel function of the first kind* (Abramowitz & Stegun, 1972, p.375), that is,

$$\mathrm{I}_d(u) \coloneqq \left(\frac{u}{2}\right)^d \sum_{i=0}^{\infty} \frac{\left(\frac{u^2}{4}\right)^i}{i!\Gamma(d + i + 1)} = \sum_{i=0}^{\infty} \frac{(u/2)^{2i+d}}{i!(i + d)!}, d \in \mathbb{Z}. \tag{4}$$

The cumulative distribution function (CDF) is

$$\Psi(u) \coloneqq \Pr\{D \leq u\} = \sum_{d=-\infty}^{\lfloor u \rfloor} e^{-(\lambda^+ + \lambda^-)} \left(\frac{\lambda^+}{\lambda^-}\right)^{\frac{d}{2}} \mathrm{I}_{|d|}\left(2\sqrt{\lambda^+\lambda^-}\right), u \in \mathbb{R}.$$

The mean and variance D are given by

$$\mathbb{E}[D] = \lambda^+ - \lambda^-, \mathrm{Var}[D] = \lambda^+ + \lambda^-.$$

In particular, for the symmetric Skellam distribution, that is, $\lambda^+ = \lambda^- \coloneqq \lambda > 0$, the PMF is simplified as

$$\Pr\{D = d; \lambda\} = e^{-2\lambda} \mathrm{I}_{|d|}(2\lambda), d \in \mathbb{Z}, \tag{5}$$

which was first derived by Irwin (1937). For example, the PMFs of Skellam distributions for a *symmetric* case $\lambda^+ = \lambda^- = 3$ and an *asymmetric* case $\lambda^+ = 2, \lambda^- = 3$ are plotted in Figure 3, respectively.

Skellam distribution has been recently adopted and modified for modeling the goal difference of two opposing teams by Karlis and Ntzoufras (2003) and high-frequency tick-by-tick discrete price changes by Koopman et al. (2017). Instead, we use it for modeling tick change $D(k) \in \mathbb{Z}$ for LPR time series (2), that is,

$$D(k) \sim \mathrm{SK}(\lambda^+, \lambda^-), k = 1, 2, ...,$$

where λ^+, λ^- can be intuitively considered as the average numbers of *potential* upward and downward tick-size jumps per month, respectively, and only the difference of upward and downward jump numbers can be observed in real world. Instead of looking at the analytical but rather complicated PMF (3), it may be more convenient to use *cumulants* to characterize stylized facts, as also adopted by, for example, R. Jarrow and Rudd (1982), Backus et al. (2011, 2014), and Martin (2013a, 2013b) for asset pricing models in finance. For example, the mean, variance, skewness and excess kurtosis of LPR level $L(t)$ can be obtained directly based on the first four cumulants as below.

Proposition 2.1 (Cumulants of LPR). *The cumulant-generating function (CGF) of the LPR level $L(t)$ based on our setting (2) is given by*

$$\ln \mathbb{E}\left[e^{vL(t)} | L(0)\right] = vL(0) + n(t)[\lambda^+(e^{bv} - 1) + \lambda^-(e^{-bv} - 1)], \tag{6}$$

the m^{th} cumulant is given by

$$\kappa_m(t) = \begin{matrix} L(0) + n(t)b\left(\lambda^+ - \lambda^-\right), m = 1, \\ n(t)b^m[\lambda^+ + (-1)^m\lambda^-], m = 2, ..., \end{matrix}$$

the mean, variance, skewness and excess kurtosis of $L(t)$ are given by

$$\mathrm{Mean}(t) = L(0) + n(t)b(\lambda^+ - \lambda^-), \tag{7}$$

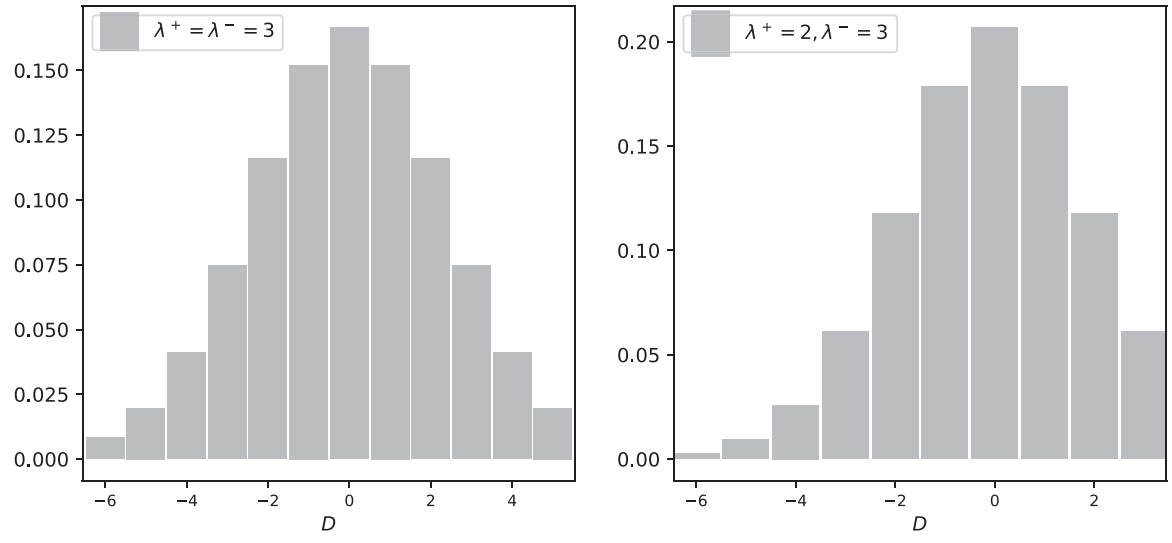

FIGURE 3 The probability mass functions of Skellam distributions $D \sim \mathrm{SK}(3, 3)$ and $D \sim \mathrm{SK}(2, 3)$

$$\begin{aligned}\text{Variance}(t) &= n(t)b^2\left(\lambda^+ + \lambda^-\right),\\ \text{Skewness}(t) &= \frac{1}{\sqrt{n(t)}}\frac{\lambda^+ - \lambda^-}{(\lambda^+ + \lambda^-)^{\frac{3}{2}}},\\ \text{ExcessKurtosis}(t) &= \frac{1}{n(t)}\frac{1}{\lambda^+ + \lambda^-}.\end{aligned} \tag{8}$$

The proof is given by Appendix A.

The skewness and (excess) kurtosis are independent of tick size b. The excess kurtosis is always positive. The distribution of $L(t)$ is positively skewed if $\lambda^+ > \lambda^-$, negatively skewed if $\lambda^+ < \lambda^-$, and symmetric if $\lambda^+ = \lambda^-$. The relationships between the Skellam-based distribution of $L(t)$ and normal distribution are summarized in Proposition 2.2. The results also help in explaining the theoretical links between our Skellam-based option pricing models and the well known Bachelier model in later sections.

Proposition 2.2 (Normal Approximation for LPR). *A normal approximation for $L(t)$ is given by*

$$L(t)|L(0) \approx^{\mathcal{D}} \mathrm{N}(L(0) + n(t)b(\lambda^+ - \lambda^-), n(t)b^2(\lambda^+ + \lambda^-)). \tag{9}$$

In particular, an asymptotics when $\lambda^+ = \lambda^- = \lambda$ is given by

$$\frac{L(t)}{b\sqrt{2\lambda n(t)}} \to^{\mathcal{D}} \mathrm{N}(0,1), t \to \infty. \tag{10}$$

Proof is provided in Appendix B.

Based on observed tick changes $\{D(k)\}_{k=1,\ldots}$, the sample mean and sample variance immediately provide a straightforward way for estimating (λ^+, λ^-) via the method of moment estimation (MME). Since

$$\hat{\mu}_D = \hat{\lambda}^+ - \hat{\lambda}^-, \mathrm{s}_D^2 = \hat{\lambda}^+ + \hat{\lambda}^-,$$

we have

$$\hat{\lambda}^+ = \frac{1}{2}\left(\mathrm{s}_D^2 + \hat{\mu}_D\right), \hat{\lambda}^- = \frac{1}{2}\left(\mathrm{s}_D^2 - \hat{\mu}_D\right),$$

where $\hat{\mu}_D$ and s_D^2 are the sample mean and sample variance of tick changes, respectively. Based on the data as presented in Figure 1, we obtain the MME-estimated potential upward and downward intensities $(\hat{\lambda}^+, \hat{\lambda}^-) = (0.5, 1.5)$ and $(\hat{\lambda}^+, \hat{\lambda}^-) = (0.0357, 0.5357)$ for the 1Y and 5Y LPRs, respectively. Alternatively, we may use the maximum likelihood estimation based on the analytical (but rather complicated) PMF (3).

3 | LPR SWAPS AND FORWARD RATES

The LPR swap market provides the key infrastructure for further development and pricing of LPR option market. The 1Y-LPR and 5Y-LPR interest rate swaps started trading on the so-called X-Swap system in August 2019. There are nine tenors including 6, 9 months and 1, 2, 3, 4, 5, 7, 10 years, and interests are paid quarterly. Quotations of swap rates are announced twice a day on 12:10 and 16:40 for bid, ask and middle prices, respectively.[7] This market data of co-initial spot swap rates can be used to obtain two important curves: *discount rate curve* (or equivalently *zero curve*), and *forward rate curve*. The former is used for

[7]For more details and historical data of LPR swap curves, see http://www.chinamoney.com.cn/chinese/bkcurvfx.

TABLE 1 The LPR swap curve on March 25, 2020

Term	3M	6M	9M	1Y	2Y	3Y	4Y	5Y	7Y	10Y
Swap rate	4.05	4.0063	3.93	3.875	3.82	3.8338	3.9	3.8325	3.95	3.95

Abbreviation: LPR, loan prime rate.

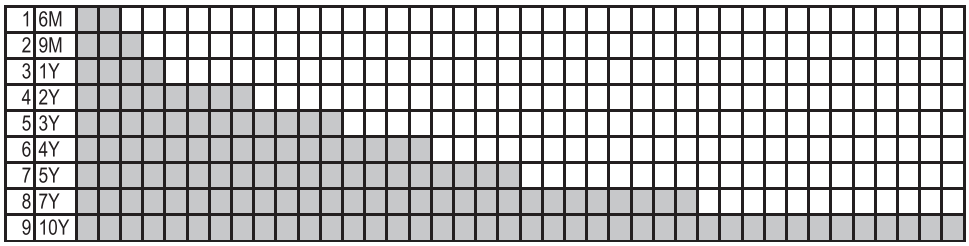

FIGURE 4 Visualization for the time grids of nine swaps (one grid one quarter)

discounting future cashflows to the present, while the latter is used for pricing interest-rate derivatives.[8] Instead of modeling the unobservable instantaneous spot rates (i.e., short rates) or instantaneous forward rates, we work directly on the LPR forward rates. The main aim of this section is to develop algorithms for construct a *simple forward LPR curve* from market-quoted swap rates, which are used as inputs in later sections for pricing interest-rate options. For clarity, let us first specify the notations and time grids for the collection of 9 co-initial spot swap rates for a given spot date t and a given type of LPR. For simplicity, we assume a unit notional amount. For the ι^{th} swap, $\iota = 1, ..., 9$, there are a set of increasing dates (i.e. a discrete *tenor structure*) $t \le T_0 < T_1 < \cdots < T_{n_\iota}$, where $T_0, ..., T_{n_\iota - 1}$ are the floating-leg reset dates, $T_1, ..., T_{n_\iota}$ are settlement (payment) dates, and T_{n_ι} is the *swap maturity* date. We denote the time grids $\mathbf{T}_\iota := \{T_0, ..., T_{n_\iota}\}$ for the ι^{th} swap covering the period $[T_0, T_{n_\iota}], \iota = 1, ..., 9$. Note that, T_0 is the common start date for all swaps, and the lengths of 9 swaps follows an increasing order as $n_1 < n_2 < \cdots < n_9$, and define $n_0 := 1$. Here, we have $n_1 = 2, n_2 = 3, n_3 = 4, n_4 = 8, n_5 = 12, n_6 = 16, n_7 = 20, n_8 = 28, n_9 = 40$ quarters for the nine LPR swaps, respectively. For example, a LPR swap curve on March 25, 2020 is provided in Table 1.

Forward tenors, the time internals between two consecutive time grids (i.e., accrual periods), are denoted by

$$\eta_j := T_j - T_{j-1}, j = 1, ..., n_9, \tag{11}$$

which are typically 3 months. *Swap tenors*, the time internals between two consecutive swap-maturity dates, are denoted by

$$\zeta_\iota := T_{n_\iota} - T_{n_{\iota-1}}, \iota = 1, ..., 9, \tag{12}$$

and we define $n_0 := 1$. For visualization, the whole structure of time grids for these nine swaps is illustrated in Figure 4, where one grid is represented as one quarter.

By definition, the ι^{th}*simple forward swap rate* $S_{0,n_\iota}(t) := S_\iota(t)$ at spot time t is set such that the spot time-t value of the ι^{th} swap covering the period $[T_0, T_{n_\iota}]$ is zero, that is,

$$P(t, T_0) - P(t, T_{n_\iota}) = S_\iota(t) \sum_{j=1}^{n_\iota} \eta_j P(t, T_j), t \in [0, T_0], \iota = 1, ..., 9, \tag{13}$$

where $P(t, T)$ is the time-t discount bond price. It is well known that, a forward swap rate can be expressed in terms of spanning simple forward rates (Brigo & Mercurio, 2006, p. 239), that is, the ι^{th} simple forward swap rate $S_\iota(t)$ in (13) can be rewritten as a nonlinear function of simple forward rates $\{F_j(t)\}_{j=1, ..., n_\iota}$, more precisely,

[8]For simplicity, we only consider the single-discounting curve framework in this paper.

$$S_\iota(t) = \frac{1 - \frac{P(t,T_{n_\iota})}{P(t,T_0)}}{\sum_{j=1}^{n_\iota} \eta_j \frac{P(t,T_j)}{P(t,T_0)}} = \frac{1 - \prod_{j=1}^{n_\iota} \frac{1}{1+\eta_j F_j(t)}}{\sum_{j=1}^{n_\iota} \eta_j \prod_{m=1}^{j} \frac{1}{1+\eta_m F_m(t)}}, t \in [0, T_0], \iota = 1, ..., 9, \tag{14}$$

where $F_j(t)$ is denoted as the *simple forward rate* for the future period $[T_{j-1}, T_j]$ prevailing at time t, that is,

$$F_j(t) := F(t; T_{j-1}, T_j) = \frac{P(t, T_{j-1}) - P(t, T_j)}{\eta_j P(t, T_j)}, t \in [0, T_{j-1}],$$

$P(t, T_{j-1})$ and $P(t, T_j)$ are time-t prices of discount bonds maturing at T_{j-1} and T_j, respectively. Note that, forward rate $F_j(t)$ coincides with the spot LPR $L(t)$ at time point T_{j-1}, that is, $F_j(T_{j-1}) = L(T_{j-1})$.

In general, a recursive relationship between *spot* swap rates $\{S_\iota(T_0)\}_{\iota=1,...,9}$ at the common start date T_0 and forward rates $\{F_j(T_0)\}_{j=1,...,n_\iota}$ is found in Proposition 3.1.

Proposition 3.1 (Swap-Forward Recursion). *A recursive relationship between the* ι^{th} *swap rate* $S_\iota(T_0)$ *and spanning forward rates* $\{F_j(T_0)\}_{j=1,...,n_\iota}$ *is given by*

$$\begin{aligned} &\left(1 - S_\iota(T_0) \sum_{j=1}^{n_{\iota-1}} \eta_j \prod_{m=1}^{j} \frac{1}{1+\eta_m F_m(T_0)}\right) \prod_{m=1}^{n_{\iota-1}} (1 + \eta_m F_m(T_0)) \\ &= \prod_{j=n_{\iota-1}+1}^{n_\iota} \frac{1}{1+\eta_j F_j(T_0)} + S_\iota(T_0) \sum_{j=n_{\iota-1}+1}^{n_\iota} \eta_j \prod_{m=n_{\iota-1}+1}^{j} \frac{1}{1+\eta_m F_m(T_0)}. \end{aligned} \tag{15}$$

The proof is provided in Appendix C.1.

As illustrated by Figure 4 for the time-grid structure of 9 swaps, the forward rates *within one year* and *beyond one year* ($1Y^+$) need to be treated separately in two different ways. More precisely, based on (15) in Proposition 3.1 and observations of spot swap rates at the common start date T_0, we can *uniquely* bootstrap all forward rates *within one year* from swaps $\iota = 1, 2, 3$ iteratively in closed forms as given by (18) in Theorem 3.1. However, the forward rates *beyond one year* cannot be uniquely bootstrapped from swaps $\iota = 4, ..., 9$ without additional assumptions, as there are more forward rates than swaps. If we further *assume* that all $1Y^+$-forward rates are piecewise-constant between two consecutive swap-maturity dates, that is,

$$F_j(T_0) = f_\iota, j = n_{\iota-1} + 1, ..., n_\iota, \iota = 4, ..., 9, \tag{16}$$

where $\{f_\iota\}_{\iota=4,...,9,}$ are constants, then, all $1Y^+$-forward rates can be *uniquely* solved numerically via (15). For notational consistence among all forward rates, we also *denote*

$$f_\iota := F_{\iota+1}(T_0), \iota = 0, 1, 2, 3, \tag{17}$$

or,

$$f_{j-1} := F_j(T_0), j = 1, 2, 3, 4.$$

Note that, $f_0 := F_1(T_0) = L(T_0)$ is known at time T_0, as this forward LPR coincides with the associated spot LPR at time T_0. Initialized by forward rate f_0, all remaining forward rates $\{f_\iota\}_{\iota=1,...,9}$ as given respectively by *assumption* (16) and *notation* (17) can be uniquely solved exactly or approximately as summarized in Theorem 3.1. For approximation,

we make a further assumption of no difference in day-count conventions, which is commonly adopted in the interest-rate literature, see e.g. Brigo and Mercurio (2006).

Theorem 3.1 (Swap-Implied Forward Curve). *Forward rate f_ι can be uniquely solved (exactly for $\iota = 1, 2, 3$, and approximately for $\iota = 4, ..., 9$) in a closed form as*

$$f_\iota = \frac{\frac{1}{\zeta_\iota} + S_\iota(T_0)}{\left(1 - S_\iota(T_0)\sum_{j=1}^{n_{\iota-1}} \eta_j \prod_{m=1}^{j} \frac{1}{1+\eta_m F_m(T_0)}\right)\prod_{m=1}^{n_{\iota-1}}\left(1+\eta_m F_m(T_0)\right)} - \frac{1}{\zeta_\iota}, \iota = 1, ..., 9. \tag{18}$$

The proof is provided in Appendix C.2.

The forward LPR curve from a straightforward implementation of Theorem 3.1 based on the swap market data on 25 March 2020 in Table 1 is plotted in Figure 5. In fact, some smoothing scheme for the forward rate curve can be further developed by bootstrapping. However, it is not the focus of this paper.

4 | PRICING LPR OPTIONS

Our key idea for pricing LPR options is to extend the classical LIBOR market model (Brace et al., 1997; Jamshidian, 1997; Miltersen et al., 1997) by replacing the lognormal distribution by the (shifted and scaled) Skellam distribution, so we denote our new model as *Skellam market model*.

4.1 | Pricing LPR caps and floors

We adopt the no-arbitrage assumption for arbitrage-free pricing in frictionless markets, or equivalently, the existence of an *equivalent martingale measure* by the fundamental theorem of asset pricing (Harrison & Kreps, 1979; Harrison & Pliska, 1981; Ross, 1978). By convention, it is much more convenient to price interest-rate options under the *forward measure* than the traditional risk-neural measure. More precisely, if we take the tradable asset T_i-bond as the *numéraire* associated with T_i-*forward measure* $\mathbb{Q}_i \sim \mathbb{P}$, then, the *simple forward rate* process $F_i(t)$ is a $\mathbb{Q}_i$-martingale. What we actually need for pricing vanilla European-type interest-rate options, such as caps and floors, is the marginal distribution at the time point T_{i-1} under the associated measure $\mathbb{Q}_i$. There are many different specifications for this distribution, such as lognormal distribution in the classical LIBOR market model. Here, to be consistent with our specification (2) under the natural probability measure $\mathbb{P}$, we assume that, under measure $\mathbb{Q}_i$,

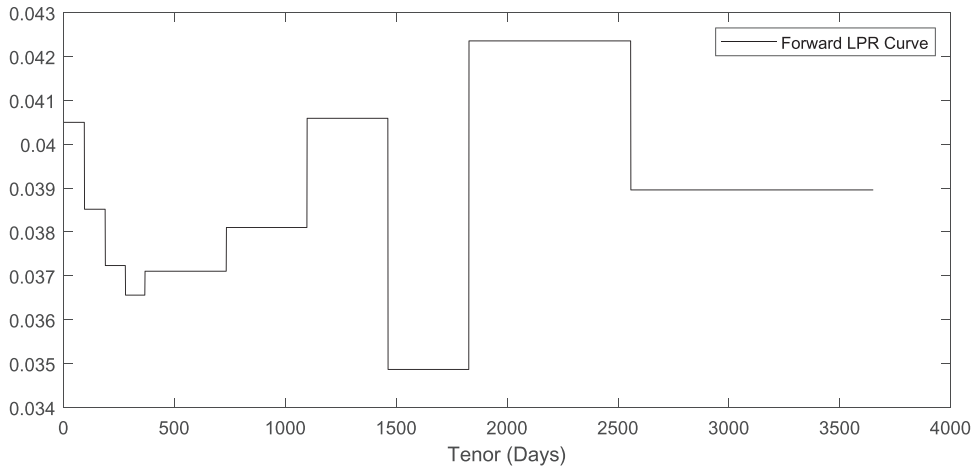

FIGURE 5 Forward LPR curve implied from market swap data on March 25, 2020 in Table 1. LPR, loan prime rate

$$L(T_{i-1}) = F_i(T_{i-1}) = F_i(0) + b\mathbf{D}_i(T_{i-1}), \tag{19}$$

where

$$\mathbf{D}_i(T_{i-1}) := \sum_{k=1}^{n(T_{i-1})} D_i(k),$$

and $\{D_i(k)\}_{k=1,\dots}$ are *i.i.d.* Skellam random variables under measure $\mathbb{Q}_i$, which is based on the *change of measure* for the sum of Skellam random variables as given by Theorem D.1 in Appendix D.

Caplets are paid in arrears. The ith caplet settles at time T_{i-1} and is paid 3 months later at time T_i. More precisely, the time-T_i payoff of the ith caplet with strike K and unit notional amount, starting at T_{i-1} and maturing at T_i is

$$\mathrm{Cpl}_i(T_i) = \eta_i(F_i(T_{i-1}) - K)^+.$$

Its current price is obtained in Theorem 4.1 as below.

Theorem 4.1 (Skellam-based LPR Caplet Price)**.** *Based on our Skellam market model* (19)*, the closed-form time-*0 *price for the ith caplet is given by*

$$\mathrm{Cpl}_i(0) = b\eta_i P(0, T_i) \sum_{d=\lceil \kappa_i \rceil}^{\infty} (d - \kappa_i) e^{-2n(T_{i-1})\lambda_i} \mathrm{I}_{|d|}(2n(T_{i-1})\lambda_i), \tag{20}$$

where $\lceil \cdot \rceil$ *is ceiling function,* $\mathrm{I}_d(\cdot)$ *is the modified Bessel function of the first kind* (4)*,*

$$\kappa_i := \frac{K - F_i(0)}{b},$$

λ_i *is the* intensity parameter *under* T_i*-forward measure* $\mathbb{Q}_i$*, and* $n(T_{i-1})$ *is the total number of LPR-announcement times within the period* $(0, T_{i-1}]$*. The proof is provided in Appendix* E.

The infinity sum in (20) can be easily calculated with high accuracy by truncation. We have only one parameter λ_i, that is, the *Skellam-implied intensity* from our pricing formula (20), just like the implied volatility from the classical Black formula. For a simple illustration, we assume $P(0, T_i) = e^{-rT_i}$ with the reference parameter setting

$$T_{i-1} = 0.25, \eta_i := T_i - T_{i-1} = 0.25, F_i(0) = K = 4\%, \lambda_i = 0.5, r = 3\%, \tag{21}$$

with the nominal amount of one million. The values of the parameters are chosen to close their real levels in market. The caplet prices generated from our Skellam market model against different parameter settings are plotted in black color in Figure 6 as a numerical study.

Given the caplet price in (20), the associated floorlet then can be priced immediately by *caplet-floorlet parity* (R. A. Jarrow & Chatterjea, 2013, p. 728). A cap (floor) is just a portfolio of caplets (floorlets) whose maturities are 3 months apart.

4.1.1 | Black-implied volatility

The world-wide industrial convention for quoting the prices of vanilla interest-rate options, such as caps/floors and swaptions, is using the *Black-implied volatility* (or *lognormal-implied volatility*) based on the standard model of log-normal market model. The Black model for interest-rate options assumes that, under the forward measure $\mathbb{Q}_i$,

$$\ln F_i(T_{i-1}) | F_i(0) \sim \mathrm{N}\left(\ln F_i(0) - \frac{1}{2}\sigma_{\mathrm{LN}}^2 T_{i-1}, \sigma_{\mathrm{LN}}^2 T_{i-1}\right),$$

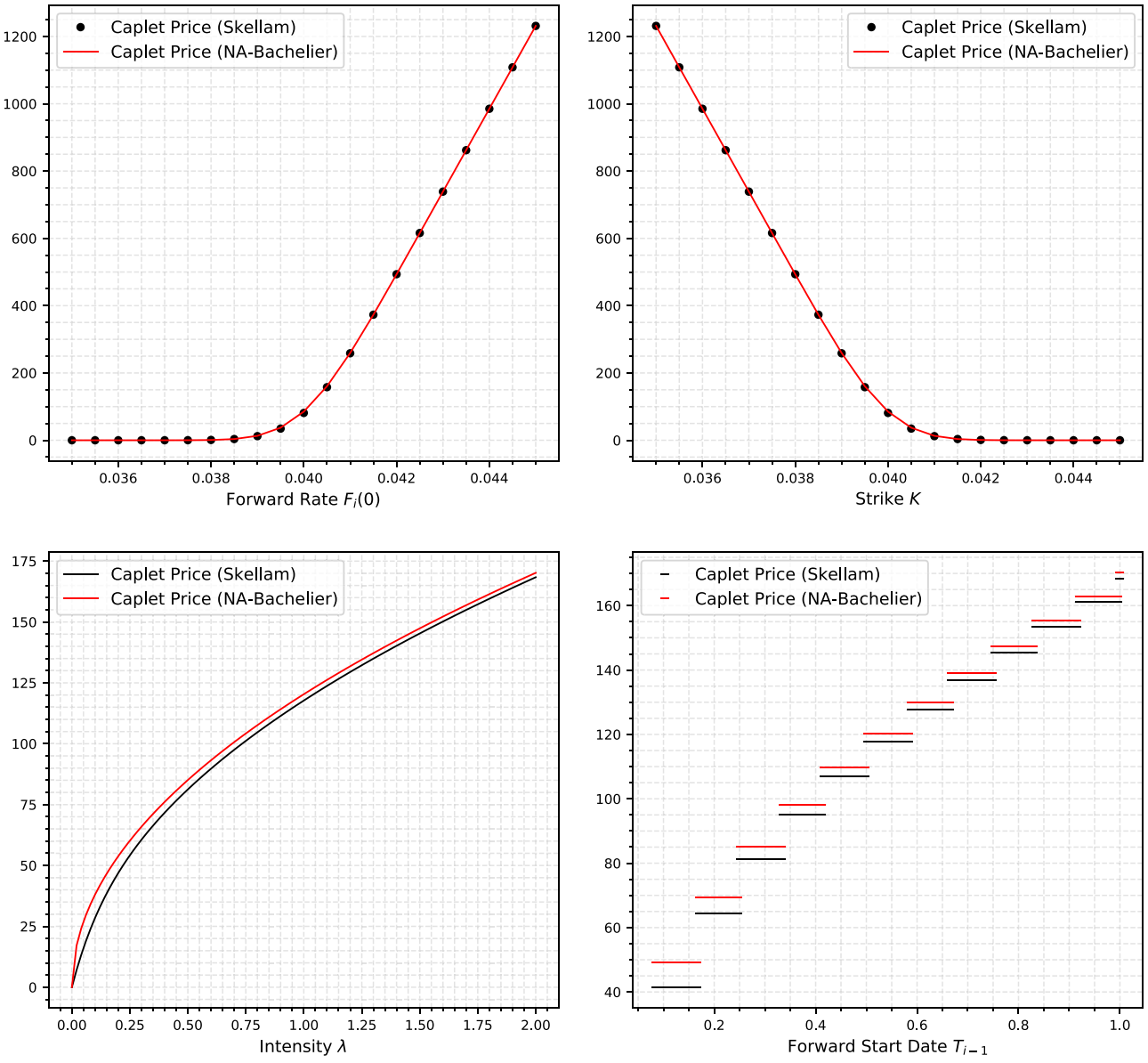

FIGURE 6 Caplet prices calculated from our Skellam model (in black color) and normal-approximated (NA) Bachelier model (in red color) against different parameter settings

where σ_{LN} is the *lognormal volatility* of $F_i(t)$. The Black formula for pricing the ith caplet is

$$\text{Cpl}_i^{\text{LN}}(0) = \eta_i P(0, T_i)(F_i(0)\Phi(d_+) - K\Phi(d_-)), \tag{22}$$

where

$$d_{\text{LN}}^{\pm} := \frac{\ln \frac{F_i(0)}{K} \pm \frac{1}{2}\sigma_{\text{LN}}^2 T_{i-1}}{\sigma\sqrt{T_{i-1}}}, d_{\text{LN}}^{+} = d_{\text{LN}}^{-} + \sigma_{\text{LN}}\sqrt{T_{i-1}},$$

and $\Phi(\cdot)$ is the CDF of the standard normal distribution $\text{N}(0, 1)$. Although it is obviously not a suitable choice for LPR options due to the absence of diffusion in the LPR time series as observed in Figure 1, let us see how the Black-implied volatility looks like from our new model. In fact, as plotted in the second graph in Figure 7 under the parameter setting (21), the Black-implied volatility from our Skellam market model presents a renowned *asymmetric* volatility smile or *volatility skew*.

4.1.2 | Bachelier-implied volatility

The simple normal market model, or Bachelier market model, recently becomes more popular in practice due to the possible presence of negative interest rates, as also advocated in e.g. Corb (2012). The normal LMM assumes that, under the forward measure $\mathbb{Q}_i$,

$$F_i(T_{i-1})|F_i(0) \sim \mathrm{N}\Big(F_i(0), \sigma_{\mathrm{N}}^2 T_{i-1}\Big), \tag{23}$$

where σ_{N} is the *normal-implied volatility* (or *Bachelier-implied volatility*) of $F_i(t)$. Then, the formula for pricing the ith caplet is given by

$$\mathrm{Cpl}_i^{\mathrm{N}}(0) = \eta_i P(0, T_i)\sigma_{\mathrm{N}}\sqrt{T_{i-1}}\,(d_{\mathrm{N}}\Phi(d_{\mathrm{N}}) + \phi(d_{\mathrm{N}})), \tag{24}$$

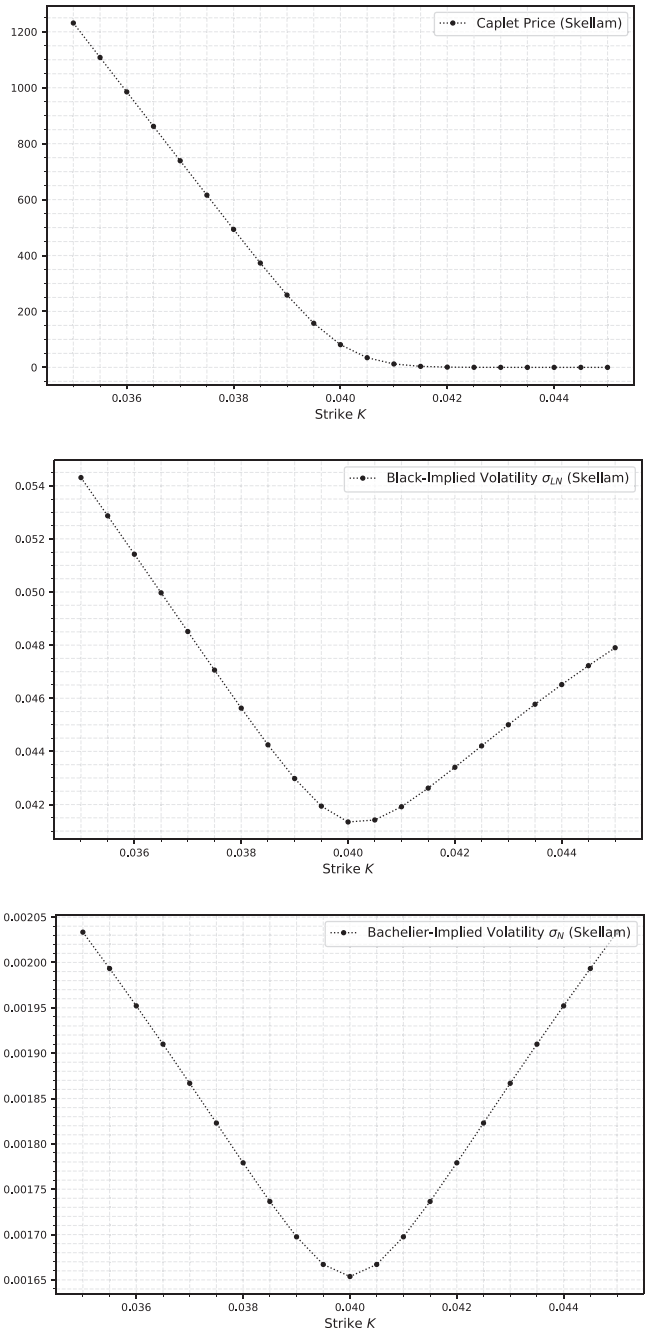

FIGURE 7 Black-implied volatility σ_{LN} and Bachelier-implied volatility σ_{N} from our Skellam market model

where

$$d_{\mathrm{N}} := \frac{F_i(0) - K}{\sigma_{\mathrm{N}}\sqrt{T_{i-1}}}, \Phi(x) := \int_{-\infty}^{x} \frac{1}{\sqrt{2\pi}} e^{-\frac{u^2}{2}} \mathrm{d}u, \phi(u) := \frac{1}{\sqrt{2\pi}} e^{-\frac{u^2}{2}}.$$

We can make a comparison with our new model via Bachelier-implied volatility as plotted in the third graph in Figure 7 under the parameter setting (21). In fact, the Bachelier-implied volatility from our Skellam market model presents a symmetric *volatility smile*. The theoretical relation between the distribution of the LPR based on Skellam model and a normal distribution is provided in Proposition 2.2, which explains this symmetry. Ignoring these stylized features of China's LPR time series as presented in Figure 1 would lead to pricing errors. More concretely, by applying the normal approximation in Proposition 2.2 to $F_i(T_{i-1})$, that is, the forward rate at the time T_{i-1} under the T_i-forward measure $\mathbb{Q}_i$, we have

$$F_i(T_{i-1})|F_i(0) \approx^{\mathcal{D}} \mathrm{N}(F_i(0), 2b^2\lambda n(T_{i-1})).$$

Then, comparing it with the normal assumption (23) by the Bachelier, and setting the two variances equal, we obtain the *Bachelier-implied volatility*

$$\sigma_{\mathrm{N}} = b\sqrt{2\lambda\frac{n(T_{i-1})}{T_{i-1}}}$$

from the *normal-approximated* Skellam model. Plugging it into the pricing formula (24) of the Bachelier, which results an analytical expression, the difference between the resulting option price $\widetilde{\mathrm{Cpl}}_i^{\mathrm{N}}(0)$ and the Skellam-generated price (20) measures the pricing error of Bachelier's model. Based on the reference parameter setting (21), the caplet prices calculated from our Skellam model (in black color) and normal-approximated (NA) Bachelier model (in red color) against different parameter settings are plotted in Figure 6, respectively. The associated pricing errors are provided in Figure 8. We can observe that, caplets are mostly overpriced using the Bachelier model, and pricing errors are large when the current forward rate is near the strike, intensity level is low, or current time is close to forward-start date. Of course, when the intensity is extremely close to zero, the option value tends to be nil, so both models agree at the origin. In particular, the mispricing is smaller when forward-start date is farther away. This is consistent *in theory* with the asymptotics (10) when time approaches to infinity and Skellam converges to Bachelier. However, *in reality*, the intensity is mostly quite small, and time is far away from infinity. In fact, only shorter-dated option contracts are liquidly traded in the market whereas very long-term options are often highly illiquid or not available at all, so, Bachelier's pricing errors cannot be generally neglected. Overall, the Bachelier model generally overprices at-the-money (ATM) and short-term options.

Finally, by summing up caplets and floorlets, the associated caps and floors are determined. Currently, standard contracts of LPR caps and floors include three terms of 6, 9 months and 1 year, with nominal amount of one million CNY and strike increments of 10 bps. Cap and floor prices are quoted by normal-implied or Bachelier-implied volatility. Based on Theorem 4.1 and the assumption of a common intensity for all tenors (i.e., *flat intensity*) for simplicity, the Skellam-implied *intensity surface* based on a very limit amount of data of market-quoted cap prices on March 26, 2020 is plotted in the left panel of Figure 9. For comparison, the associated Bachelier-implied volatility surface is plotted on the right. In particular, for example, within 9-month time to maturity, both Skellam-implied intensity and Bachelier-implied volatility present smile (*frown*) (see Figure 10).

4.2 | Pricing LPR swaption

The ι^{th} simple forward swap rate $S_{0,n_\iota}(t) := S_\iota(t)$ as implied by (13) for $t \in [0, T_0]$ can be expressed as

$$S_\iota(t) = \frac{P(t, T_0) - P(t, T_{n_\iota})}{A_\iota(t)}, t \in [0, T_0], \iota = 1, ..., 9,$$

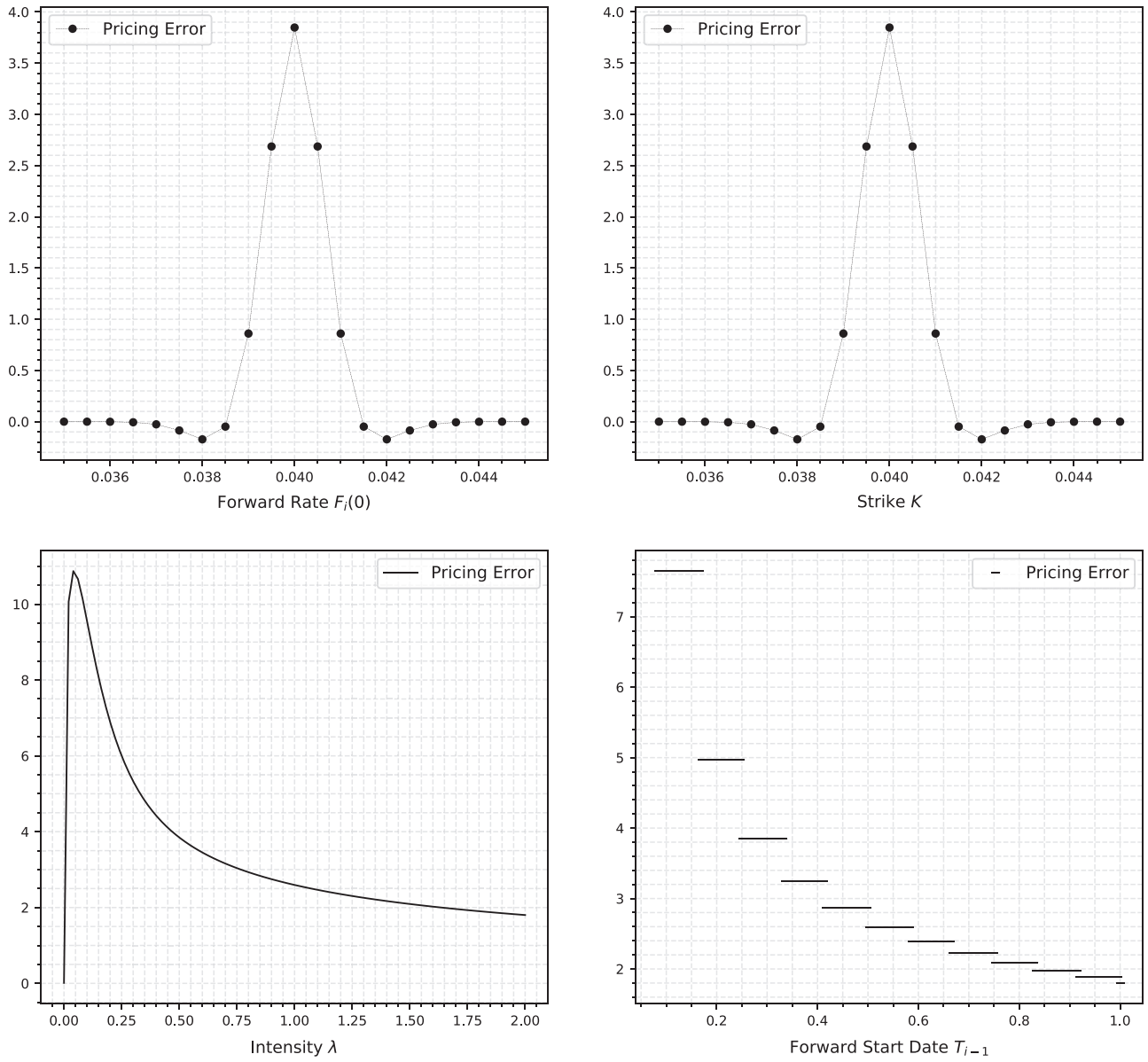

FIGURE 8 Caplet pricing errors of normal-approximated Bachelier model against different parameter settings

where $A_\iota(t)$ is the *swap annuity* or *present value of basis point* (PVBP), that is,

$$A_\iota(t) := \sum_{j=1}^{n_\iota} \eta_j P(t, T_j),$$

and it can be considered as a tradable asset. Then, we can take it as the *numéraire* associated with *forward-swap measure* $\mathbb{S}_\iota$, and $S_\iota(t)$ is a $\mathbb{S}_\iota$-martingale. Moreover, it is well known that, the simple forward swap rate (14) can be alternatively interpreted as a weighted linear combination of spanning forward rates and can be approximated by *weight freezing* at time 0, that is,

$$S_\iota(t) = \sum_{j=1}^{n_\iota} w_j(t) F_j(t) \approx \sum_{j=1}^{n_\iota} w_j(0) F_j(t),$$

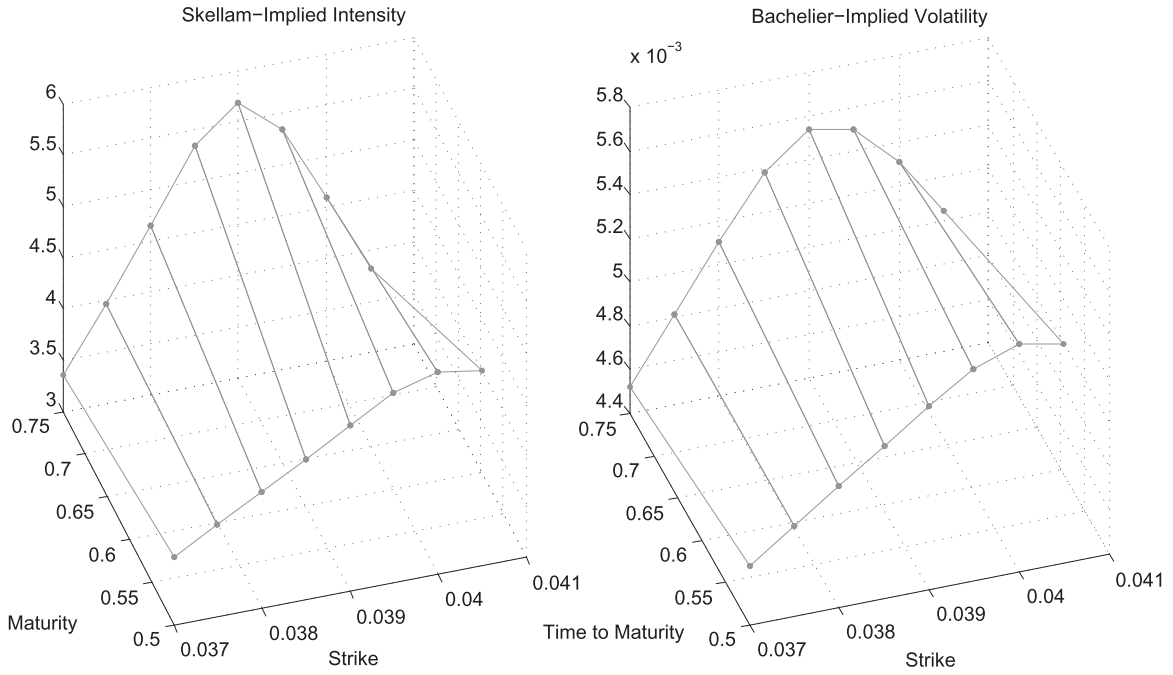

FIGURE 9 Skellam-implied *intensity surface* and Bachelier-implied *volatility surface* from market-quoted cap prices on March 26, 2020

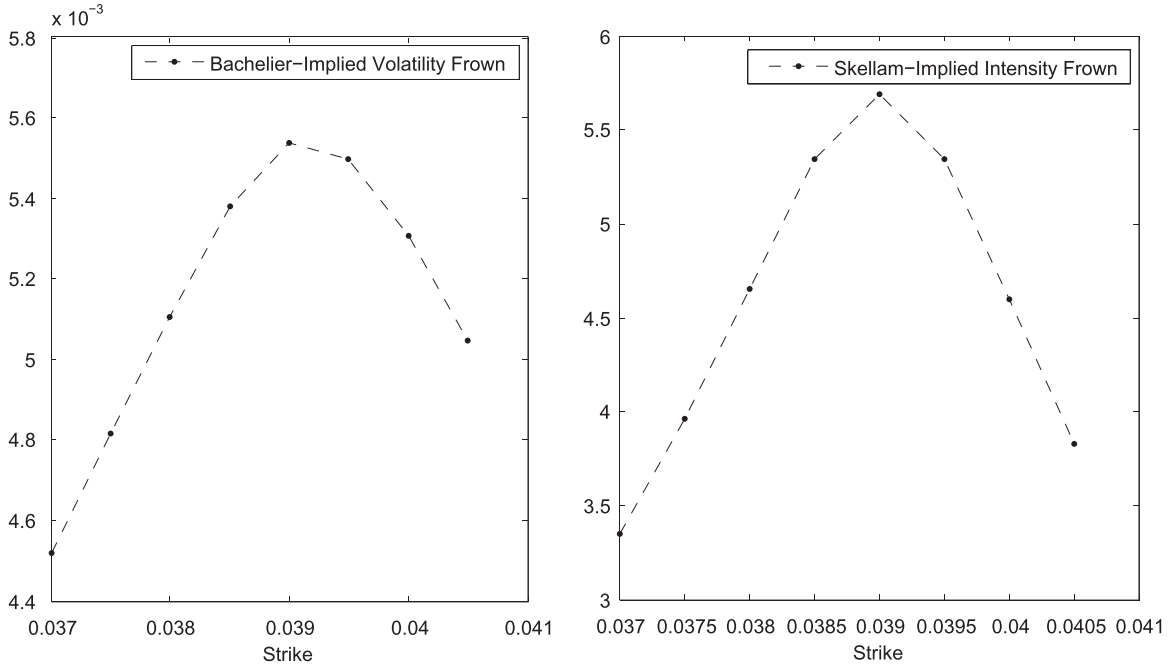

FIGURE 10 Skellam-implied *intensity frown* and Bachelier-implied *volatility frown* from market-quoted 9-month cap prices on March 26, 2020

where

$$w_j(t) := \frac{\eta_j P(t, T_j)}{\sum_{m=1}^{n_i} \eta_m P(t, T_m)}.$$

Rebonato (1998) found that the variability of weights is small in comparison with the variability of forwards, so the weight terms can be approximated by their initial values. In fact, this *weight freezing* approach provides a reasonable approximation, and empirically it has been validated intensively in the literature and widely adopted by the industry, see also (Brigo & Mercurio, 2006, §8). To be consistent with our previous assumption in (19), we have

$$F_j(T_0) = F_j(0) + b\mathbf{D}_j(T_0), j = 1, ..., n_\iota,$$

then,

$$\begin{aligned} S_\iota(T_0) &\approx \sum_{j=1}^{n_\iota} w_j(0) F_j(T_0) \\ &= S_{n_\iota}(0) + b\sum_{j=1}^{n_\iota} w_j(0)\mathbf{D}_j(T_0), \end{aligned} \tag{25}$$

where

$$\mathbf{D}_j(T_0) := \sum_{k=0}^{n(T_0)} D_j(k),$$

and $\{D_j(k)\}_{k=1,\ldots}$ are *i.i.d.* Skellam random variables, and $D_j(0) := 0$. So, similarly, we assume that,

$$S_{n_\iota}(T_0) = S_{n_\iota}(0) + b\mathbf{D}^{\mathbb{S}_\iota}(T_0), \tag{26}$$

where

$$\mathbf{D}^{\mathbb{S}_\iota}(T_0) := \sum_{k=0}^{n(T_0)} D^{\mathbb{S}_\iota}(k),$$

and $\{D^{\mathbb{S}_\iota}(k)\}_{k=1,\ldots}$ are *i.i.d.* Skellam random variables under measure $\mathbb{S}_\iota$, and $D^{\mathbb{S}_\iota}(0) := 0$. We can show that, the distributions of (25) and (26) are approximatively the same, see the proof in Appendix F.

Swaption is an European call or put option on interest rate swap. The *swaption maturity* is the first reset date T_0 of the underlying interest rate swap, and the holder of *payer swaption* has the right (but not the obligation) to enter a *payer swap* at T_0. The payoff of the ι^{th} payer swaption (i.e. T_0-*into*-$(T_{n_\iota} - T_0)$ *swaption*, or $T_0 \times (T_{n_\iota} - T_0)$ *swaption*) with strike K and unit notional amount at the swaption maturity T_0 is

$$\text{PSwpt}_\iota(T_0) = (S_{n_\iota}(T_0) - K)^+ \sum_{j=1}^{n_\iota} \eta_j P(T_0, T_j).$$

Its current price in analytical form is provided in Corollary 4.1 as below.

Corollary 4.1 (Skellam-based LPR Swaption Price)**.** *Based on our Skellam swap market model* (26)*, the closed-form time-0 price for the ιth payer swaption is given by*

$$\text{PSwpt}_\iota(0) = bA_\iota(0) \sum_{d=\lceil \kappa_\iota \rceil}^{\infty} (d - \kappa_\iota) e^{-2n(T_0)\lambda^{\mathbb{S}_\iota}} \mathrm{I}_{|d|}(2n(T_0)\lambda^{\mathbb{S}_\iota}), \tag{27}$$

where $\lceil \cdot \rceil$ *is ceiling function,* $\mathrm{I}_d(\cdot)$ *is the modified Bessel function of the first kind* (4)*,*

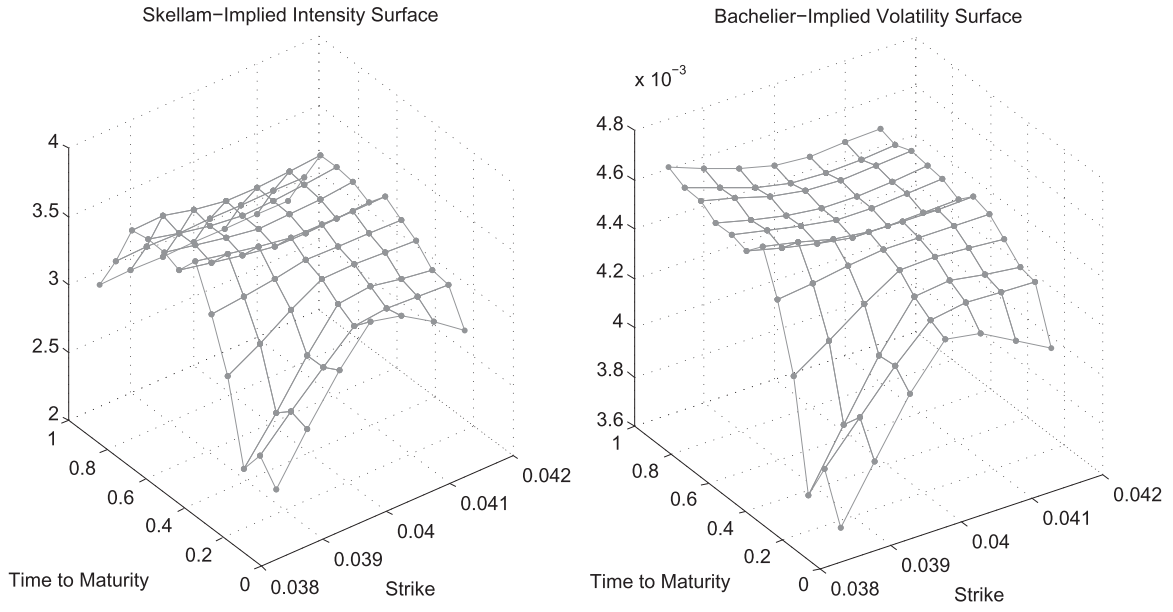

FIGURE 11 Skellam-implied *intensity surface* and Bachelier-implied *volatility surface* from market-quoted 6-month swaption prices on March 26, 2020

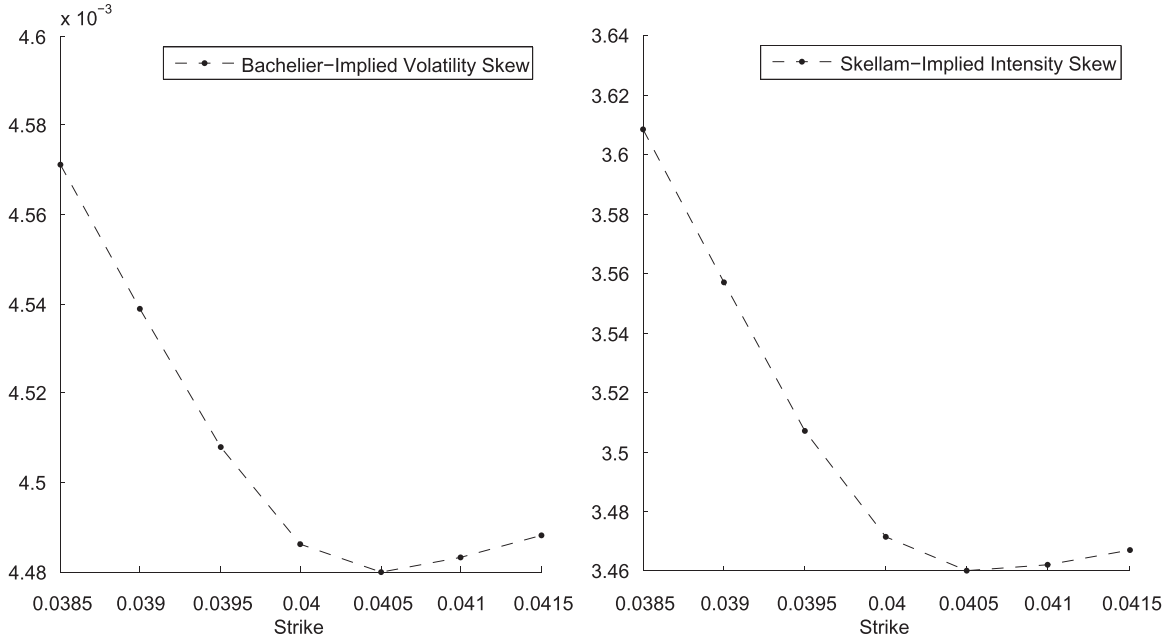

FIGURE 12 Skellam-implied *intensity skew* and Bachelier-implied *volatility skew* from market-quoted 6-month swaption prices with 6-month time to maturity on March 26, 2020

$$\kappa_t := \frac{K - S_t(0)}{b},$$

$\lambda^{\mathbb{S}_t}$ is the rate parameter *under forward-swap measure $\mathbb{S}_t$, and $n(T_0)$ is the total number of LPR-announcement times within the period $(0, T_0]$. The proof is provided in Appendix G.*

Currently, standard contracts of LPR swaptions include five terms of 1, 3, 6, 9 months and 1 year, with nominal amount of one million CNY and strike increments of either 5 or 10 bps. Swaption prices are quoted by normal-implied or Bachelier-implied swap volatility. Based on Corollary 4.1, the Skellam-implied *intensity surface* based on a very limit

amount of data of market-quoted 6-month swaption prices on March 26, 2020 is plotted on the left panel of Figure 11. For comparison, the associated Bachelier-implied volatility surface is plotted on the right. In particular, for example, with 6-month time to maturity, both Skellam-implied intensity and Bachelier-implied volatility present smile (skew) (see Figure 12). This preliminary empirical result of *intensity skew* implied from swaptions, together with *intensity frown* implied from caps as seen in Figure 12, shows that, our Skellam-based market model, similarly as the normal-based Bachelier model or lognormal-based Black model, cannot fully capture the real data just by using a single parameter, although it is consistent with the LPR time series as observed in Figure 1. This early warning enlightens future investigations and model extensions for future research.

4.3 | Discussions: Black, Bachelier and Skellam

These three models (i.e., the market standard model of Black, the increasingly popular model of Bachelier, and our newly-introduced model of Skellam) are all *two-parameter* models in the natural world and *single-parameter* models in the risk-neutral world. So in theory they offer the same degree of flexibility, and almost have a 1-1 correspondence between each other. Now, it is quite fair for us to make comparisons among them. Both the Black and the Bachelier are *pure-diffusion* models, whereas the Skellam is a *pure-jump* model.

Historically, the Black model takes over the Bachelier model as the market standard, mainly due to the fact that the latter has a fatal flaw of possibly generating negative interest rate. However, this traditional argument may soon become a history, as nowadays negative interest rates are possible in the real world (e.g., Japan) and even more ubiquitous. The Bachelier's ability to generate negative interest rates now becomes an advantage over the Black. In addition, it can also generate the implied-volatility *skew* for option pricing. So it is an increasingly popular model in the industry recently, as also advocated by leading practitioners, for example, Corb (2012).

Fortunately, our Skellam model retains both advantages of the Bachelier: possibilities for negative interest rates and implied-volatility *skew* (as presented in Figure 7). In theory, the Bachelier model can be considered as a special case, the limiting version (as proved in Proposition 2.2), of our Skellam model. Moreover, our Skellam model offers some extra advantages over the Bachelier: the former can generate *asymmetric* distributions for the LPRs with positive or negative skewness when the potential upward and downward intensities are nonidentical, that is, $\lambda^+ \neq \lambda^-$ (as proved in Proposition 2.1), whereas the latter is normal and can only generate *symmetric* distributions. The time series of both 1Y and 5Y LPRs currently have clear downward trends as presented in Figure 1. The associated sample skewnesses, MME-estimated potential upward and downward intensities of monthly 1Y and 5Y LPRs are $-1.4842, -1.2288$, $(\lambda^+, \lambda^-) = (0.5, 1.5), (0.0357, 0.5357)$, respectively. The potential downward intensities are much larger than the upward ones, which capture the significantly negatively skewed feature of LPR time series in actual data. Therefore, Bachelier's model is insufficient here. Finally, the Skellam is the only model of the three that can capture these stylized features (such as state discreteness and timing fixation) of China's LPR time series as presented in Figure 1. Inability to take into account these crucial features may lead to sizable mispricing as demonstrated in Section 4.1 and Figure 8, and traditional models such as the Bachelier are not safe to use in general. So among these three *parametrically parsimonious* models equipped with the same number of parameters, it shall be fair for us to make a claim that our Skellam model is superior to traditional models of Black and Bachelier at least in the current China's LPR market.

5 | CONCLUDING REMARKS

China's LPR time series present some unique features of the randomness which cannot be captured appropriately by existing models for interest-rate options in the literature. Our key finding of great interest in general is that, different from traditional options, the risk-neutral intensity (rather than diffusion) plays a dominant role in pricing these new LPR derivatives, which resemble the more familiar credit derivatives. In this paper, we introduced *Skellam market model*, a novel market model based on the integer-valued Skellam distribution, for modeling LPR time series and pricing vanilla LPR options in analytical forms. Our primary aim of this paper is to develop a parametrically parsimonious *continuous-time* model in the simplest possible setting that can capture key features of LPR, and could serve as a benchmark easily implementable in practice, parallelly with current market standards of Black's lognormal and Bachelier's normal market models. To be consistent with our observation typically as Figure 1, we advocate that it is more meaningful to quote LPR option prices in terms of the *implied intensity* rather than the conventional implied volatility. Indeed, there is virtually no

diffusion component in the underlying at all. This consistence is important, as it would facilitate more efficient risk management and more accurate option-implied forward-looking analysis. This new model is first applied to China's interest-rate options market, and it is of course extendable for other markets if the underlying of traded options would present similar features. In fact, this model allows numerous potential extensions with multiple factors, time-varying jump rates, the difference of two more general count models (such as *doubly stochastic Poisson* or *Cox* models with randomized intensities) and multiple-discounting curves, which may serve better in explaining more real data of LPR time series and option prices, such as Skellam-implied *intensity smile*, that is, the *intensity frown* implied from caps and *intensity skew* implied from swaptions as presented in Figures 10 and 12, respectively. Obvious extensions for addressing these issues are *local intensity* and *stochastic intensity* models, parallelly with existing voluminous literature on local volatility and stochastic volatility models. At this moment, however, we only have a short history of LPR time series and a very limited amount of LPR option data, and comprehensive empirical studies associated with these models would surely follow once longer spans of data become available. They are all proposed for future research.

ACKNOWLEDGMENTS

The authors would like to thank Robert Webb (editor) and reviewers for very constructive comments and suggestions that greatly improved the presentation of our results. The corresponding author Hongbiao Zhao would like to acknowledge the financial support from the *National Natural Science Foundation of China* (#71401147) and the research fund provided by the Innovative Research Team of *Shanghai University of Finance and Economics* (#2020110930) and *Shanghai Institute of International Finance and Economics*.

DATA AVAILABILITY STATEMENT

Spot LPR and LPR swap data are publicly available at the website of the National Interbank Funding Center (NIFC): Spot LPR data: http://www.chinamoney.com.cn/chinese/bklpr and LPR swap data: http://www.chinamoney.com.cn/chinese/bkcurvfx.

ORCID


Hongbiao Zhao https://orcid.org/0000-0002-1698-8434

REFERENCES

Abramowitz, M., & Stegun, I. A. (1972). *Handbook of mathematical functions: With formulas, graphs, and mathematical tables*. Dover.

Amstad, M., & He, Z. (2020). Chapter 5: Chinese bond market and interbank market. In M. Amstad, G. Sun, & W. Xiong (Eds.), *The handbook of China's financial system* (105–150). Princeton University Press.

Andersen, L., & Andreasen, J. (2000). Volatility skews and extensions of the LIBOR market model. *Applied Mathematical Finance*, *7*(1), 1–32.

Andersen, L. B., & Brotherton-Ratcliffe, R. (2001). *Extended LIBOR market models with stochastic volatility* (working paper). Gen Re Securities.

Backus, D., Chernov, M., & Martin, I. (2011). Disasters implied by equity index options. *Journal of Finance*, *66*(6), 1969–2012.

Backus, D., Chernov, M., & Zin, S. (2014). Sources of entropy in representative agent models. *Journal of Finance*, *69*(1), 51–99.

Barndorff-Nielsen, O. E., Pollard, D. G., & Shephard, N. (2012). Integer-valued Lévy processes and low latency financial econometrics. *Quantitative Finance*, *12*(4), 587–605.

Bates, D. S. (1996). Chapter 20: Testing option pricing models. In G. Maddala, & C. R. Rao (Eds.), *Handbook of statistics: Statistical methods in finance* (Vol. 14, pp. 567–611). Elsevier.

Brace, A., Gatarek, D., & Musiela, M. (1997). The market model of interest rate dynamics. *Mathematical Finance*, *7*(2), 127–155.

Brigo, D., & Mercurio, F. (2006). *Interest rate models—Theory and practice: With smile, inflation and credit* (2nd ed.). Springer.

Carr, P. (2011). Semi-static hedging of barrier options under Poisson jumps. *International Journal of Theoretical and Applied Finance*, *14*(7), 1091–1111.

Clarida, R., Galí, J., & Gertler, M. (2000). Monetary policy rules and macroeconomic stability: evidence and some theory. *Quarterly Journal of Economics*, *115*(1), 147–180.

Cochrane, J. H., & Piazzesi, M. (2002). The Fed and interest rates—A high-frequency identification. *American Economic Review*, *92*(2), 90–95.

Corb, H. (2012). *Interest Rate Swaps and Other Derivatives*. Columbia University Press.

Cox, J. C., Ingersoll Jr., J. E., & Ross, S. A. (1985). A theory of the term structure of interest rates. *Econometrica*, *53*(2), 385–407.

Dubinsky, A., Johannes, M., Kaeck, A., & Seeger, N. J. (2019). Option pricing of earnings announcement risks. *Review of Financial Studies*, *32*(2), 646–687.

Duffie, D., & Stein, J. C. (2015). Reforming LIBOR and other financial market benchmarks. *Journal of Economic Perspectives*, *29*(2), 191–212.

Eberlein, E., & Özkan, F. (2005). The Lévy LIBOR model. *Finance and Stochastics*, *9*(3), 327–348.

Glasserman, P., & Kou, S. G. (2003). The term structure of simple forward rates with jump risk. *Mathematical Finance*, *13*(3), 383–410.

Hagan, P. S., Kumar, D., Lesniewski, A. S., & Woodward, D. E. (2002, September). Managing smile risk. *Wilmott Magazine*, 84–108.

Hamilton, J. D., & Jordà, O. (2002). A model of the federal funds rate target. *Journal of Political Economy*, *110*(5), 1135–1167.
Han, B. (2007). Stochastic volatilities and correlations of bond yields. *Journal of Finance*, *62*(3), 1491–1524.
Harrison, J. M., & Kreps, D. M. (1979). Martingales and arbitrage in multiperiod securities markets. *Journal of Economic Theory*, *20*(3), 381–408.
Harrison, J. M., & Pliska, S. R. (1981). Martingales and stochastic integrals in the theory of continuous trading. *Stochastic Processes and their Applications*, *11*(3), 215–260.
Heath, D., Jarrow, R., & Morton, A. (1992). Bond pricing and the term structure of interest rates: A new methodology for contingent claims valuation. *Econometrica*, *60*(1), 77–105.
Irwin, J. O. (1937). The frequency distribution of the difference between two independent variates following the same Poisson distribution. *Journal of the Royal Statistical Society*, *100*(3), 415–416.
Jamshidian, F. (1997). LIBOR and swap market models and measures. *Finance and Stochastics*, *1*(4), 293–330.
Jarrow, R., Li, H., & Zhao, F. (2007). Interest rate caps "smile" too! but can the LIBOR market models capture the smile? *Journal of Finance*, *62*(1), 345–382.
Jarrow, R., & Rudd, A. (1982). Approximate option valuation for arbitrary stochastic processes. *Journal of Financial Economics*, *10*(3), 347–369.
Jarrow, R. A., & Chatterjea, A. (2013). *An introduction to derivative securities, financial markets, and risk management*. WW Norton & Company.
Joshi, M. S., & Rebonato, R. (2003). A displaced-diffusion stochastic volatility LIBOR market model: motivation, definition and implementation. *Quantitative Finance*, *3*(6), 458–469.
Karlis, D., & Ntzoufras, I. (2003). Analysis of sports data by using bivariate Poisson models. *Journal of the Royal Statistical Society: Series D (The Statistician)*, *52*(3), 381–393.
Kim, D. H., & Wright, J. H. (2016). *Jumps in bond yields at known times* (technical report). National Bureau of Economic Research.
Koopman, S. J., Lit, R., & Lucas, A. (2017). Intraday stochastic volatility in discrete price changes: the dynamic Skellam model. *Journal of the American Statistical Association*, *112*(520), 1490–1503.
Leippold, M., & Strømberg, J. (2014). Time-changed Lévy LIBOR market model: Pricing and joint estimation of the cap surface and swaption cube. *Journal of Financial Economics*, *111*(1), 224–250.
Martin, I. (2013a). The lucas orchard. *Econometrica*, *81*(1), 55–111.
Martin, I. W. (2013b). Consumption-based asset pricing with higher cumulants. *Review of Economic Studies*, *80*(2), 745–773.
Miltersen, K. R., Sandmann, K., & Sondermann, D. (1997). Closed form solutions for term structure derivatives with log-normal interest rates. *Journal of Finance*, *52*(1), 409–430.
Piazzesi, M. (2001, April). *An econometric model of the yield curve with macroeconomic jump effects* (Working Paper No. 8246). Cambridge, MA: NBER.
Piazzesi, M. (2005). Bond yields and the federal reserve. *Journal of Political Economy*, *113*(2), 311–344.
Piazzesi, M. (2010). Affine term structure models. In Y. Aït-Sahalia, & L. P. Hansen (Eds.), *Handbook of financial econometrics: Tools and techniques* (Vol. 1, pp. 691–766). Elsevier.
Rebonato, R. (1998). *Interest rate option models* (2nd ed.). John Wiley & Sons.
Ross, S. A. (1978). A simple approach to the valuation of risky streams. *Journal of Business*, *51*(3), 453–475.
Sato, K.-I. (1999). *Lévy processes and infinitely divisible distributions*. Cambridge University Press, Cambridge.
Schipke, M. A., Rodlauer, M. M., & Zhang, M. L. (2019). *The future of China's bond market*. International Monetary Fund.
Skellam, J. G. (1946). The frequency distribution of the difference between two Poisson variates belonging to different populations. *Journal of the Royal Statistical Society Series A (General)*, *109*(3), 296.
The National Interbank Funding Center (NIFC).http://www.chinamoney.com.cn

How to cite this article: Chen, Z., Zhang, K., & Zhao, H. (2022). A Skellam market model for *loan prime rate* options. *Journal of Futures Markets*, 42, 525–551. https://doi.org/10.1002/fut.22273

APPENDIX A: PROOF FOR PROPOSITION 2.1

Proof. Based on our model (2), it is straightforward to obtain the mean by

$$\mu_1(t) := \mathbb{E}[L(t)] = L(0) + b\sum_{k=0}^{n(t)} \mathbb{E}[D(k)] = L(0) + n(t)b(\lambda^+ - \lambda^-). \tag{A1}$$

Note that, $D(0) := 0$. To fully characterize the distributional properties, let's us derive the transformation functions for $L(t)$. The the moment-generating functions (MGFs) of N^+, N^- are

$$\mathbb{E}\left[e^{vN^+}\right] = \exp(\lambda^+(e^v - 1)), \mathbb{E}\left[e^{vN^-}\right] = \exp(\lambda^-(e^v - 1)),$$

then, the MGF of D is

$$\mathbb{E}[e^{vD}] = \mathbb{E}\left[e^{v(N^+ - N^-)}\right] = \exp(\lambda^+(e^v - 1) + \lambda^-(e^{-v} - 1)).$$

So, the MGF of $L(t)$ is

$$\begin{aligned}\mathbb{E}[e^{vL(t)}|L(0)] = & \quad e^{vL(0)}\mathbb{E}\left[\prod_{k=1}^{n(t)}\exp(vbD(k))\right] \\ & = \exp(vL(0) + n(t)[\lambda^+(e^{bv} - 1) + \lambda^-(e^{-bv} - 1)]),\end{aligned}$$

and the cumulant-generating function (CGF) is given by

$$\mathrm{K}(v, t) := \ln\mathbb{E}[e^{vL(t)}|L(0)] = vL(0) + n(t)[\lambda^+(e^{bv} - 1) + \lambda^-(e^{-bv} - 1)].$$

Then, we can derive any cumulant by

$$\kappa_m(t) = \left.\frac{\partial^m \mathrm{K}(v, t)}{\partial v^m}\right|_{v=0}, m \in \mathbb{N}^+,$$

where $\kappa_m(t)$ is the m^{th} cumulant. Then, we have

$$\text{mean} = \kappa_1(t), \text{ variance} = \kappa_2(t), \text{ skewness} = \frac{\kappa_3(t)}{\kappa_2^{\frac{3}{2}}(t)}, \text{ excess kurtosis} = \frac{\kappa_4(t)}{\kappa_2^2(t)}.$$

For the first cumulant, we have

$$\kappa_1(t) = \left.\frac{\partial \mathrm{K}(v, t)}{\partial v}\right|_{v=0} = L(0) + n(t)b(\lambda^+ - \lambda^-).$$

It is easy to find a similar structure for any higher-order cumulants analytically as summarized by

$$\kappa_m(t) = \left.\frac{\partial^m \mathrm{K}(v, t)}{\partial v^m}\right|_{v=0} = L(0)\mathbf{1}_{\{m=1\}} + n(t)b^m[\lambda^+ + (-1)^m\lambda^-], m \in \mathbb{N}^+.$$

Then, we can easily obtain the mean, variance, skewness and excess kurtosis as given by Proposition 2.1. □

APPENDIX B: PROOF FOR PROPOSITION 2.2

Proof. It is easy to look at their distributional links via their probability transform functions. Based on the CGF (6), simply replacing v by $\frac{v}{b\sqrt{n(t)}}$, we have the CGF of $\frac{L(t)}{b\sqrt{n(t)}}$,

$$\begin{aligned}& \ln\mathbb{E}\left[e^{\frac{L(t)}{b\sqrt{n(t)}}v}|L(0)\right] \\ = & \frac{L(0)}{b\sqrt{n(t)}}v + n(t)\left[\lambda^+\left(e^{\frac{v}{\sqrt{n(t)}}} - 1\right) + \lambda^-\left(e^{-\frac{v}{\sqrt{n(t)}}} - 1\right)\right] \\ = & \frac{L(0)}{b\sqrt{n(t)}}v \\ & + \lambda^+\left(v\sqrt{n(t)} + \frac{1}{2}v^2 + \sum_{i=2}^{\infty}\frac{v^i}{i!}(n(t))^{1-\frac{i}{2}}\right) + \lambda^-\left(-v\sqrt{n(t)} + \frac{1}{2}v^2 + \sum_{i=2}^{\infty}\frac{v^i}{i!}(-1)^i(n(t))^{1-\frac{i}{2}}\right),\end{aligned} \tag{B1}$$

where by applying the Taylor's expansion to exponential functions,

$$e^{\frac{v}{\sqrt{n(t)}}} = 1 + \frac{v}{\sqrt{n(t)}} + \frac{1}{2}\frac{v^2}{n(t)} + \sum_{i=2}^{\infty}\frac{1}{i!}\left(\frac{v}{\sqrt{n(t)}}\right)^i, e^{-\frac{v}{\sqrt{n(t)}}} = 1 - \frac{v}{\sqrt{n(t)}} + \frac{1}{2}\frac{v^2}{n(t)} + \sum_{i=2}^{\infty}\frac{1}{i!}\left(-\frac{v}{\sqrt{n(t)}}\right)^i.$$

By ignoring relatively small terms in the expansion (B1),

$$\begin{aligned}\ln\mathbb{E}\left[e^{\frac{L(t)}{b\sqrt{n(t)}}v}|L(0)\right] &\approx \frac{L(0)}{b\sqrt{n(t)}}v + \lambda^+\left(v\sqrt{n(t)} + \frac{1}{2}v^2\right) + \lambda^-\left(-v\sqrt{n(t)} + \frac{1}{2}v^2\right)\\ &= \left(\frac{L(0)}{b\sqrt{n(t)}} + \sqrt{n(t)}\lambda^+ - \sqrt{n(t)}\lambda^-\right)v + \frac{1}{2}v^2(\lambda^+ + \lambda^-),\end{aligned}$$

we can also find a normal approximation,

$$\frac{L(t)}{b\sqrt{n(t)}}|L(0) \approx^{\mathcal{D}} \mathrm{N}\left(\frac{L(0)}{b\sqrt{n(t)}} + \sqrt{n(t)}\lambda^+ - \sqrt{n(t)}\lambda^-, \lambda^+ + \lambda^-\right),$$

or, (9). In particular, if the distribution is symmetric, that is, $\lambda^+ = \lambda^- = \lambda$, then, based on the expansion (B1), we have

$$\ln\mathbb{E}\left[e^{\frac{L(t)}{b\sqrt{n(t)}}v}|L(0)\right] = \frac{L(0)}{b\sqrt{n(t)}}v + \lambda\left(v^2 + \sum_{i=2}^{\infty}\frac{v^i}{i!}(n(t))^{1-\frac{i}{2}} + \sum_{i=2}^{\infty}\frac{v^i}{i!}(-1)^i(n(t))^{1-\frac{i}{2}}\right).$$

If $t \to \infty$, then, $n(t) \to \infty$ and

$$\lim_{t\to\infty}\ln\mathbb{E}\left[e^{\frac{L(t)}{b\sqrt{n(t)}}v}|L(0)\right] = \lambda v^2,$$

which implies a normal distribution $\mathrm{N}(0, 2\lambda)$. So, we have (10). □

APPENDIX C: PROOFS FOR SWAP-IMPLIED FORWARD CURVE

Proof for Proposition 3.1

Proof. By (14), we have

$$S_l(T_0) = \frac{1 - \prod_{j=1}^{n_l}\frac{1}{1+\eta_j F_j(T_0)}}{\sum_{j=1}^{n_l}\eta_j\prod_{m=1}^{j}\frac{1}{1+\eta_m F_m(T_0)}},$$

$$S_l(T_0)\left(\sum_{j=1}^{n_{l-1}}\eta_j\prod_{m=1}^{j}\frac{1}{1+\eta_m F_m(T_0)} + \sum_{j=n_{l-1}+1}^{n_l}\eta_j\prod_{m=1}^{j}\frac{1}{1+\eta_m F_m(T_0)}\right) = 1 - \prod_{j=1}^{n_{l-1}}\frac{1}{1+\eta_j F_j(T_0)}\prod_{j=n_{l-1}+1}^{n_l}\frac{1}{1+\eta_j F_j(T_0)}.$$

Note that,

$$\sum_{j=n_{\iota-1}+1}^{n_\iota}\eta_j\prod_{m=1}^{j}\frac{1}{1+\eta_m F_m(T_0)}=\prod_{m=1}^{n_{\iota-1}}\frac{1}{1+\eta_m F_m(T_0)}\sum_{j=n_{\iota-1}+1}^{n_\iota}\eta_j\prod_{m=n_{\iota-1}+1}^{j}\frac{1}{1+\eta_m F_m(T_0)},$$

then, we obtain

$$\begin{aligned}&\prod_{j=1}^{n_{\iota-1}}\frac{1}{1+\eta_j F_j(T_0)}\prod_{j=n_{\iota-1}+1}^{n_\iota}\frac{1}{1+\eta_j F_j(T_0)}+S_\iota(T_0)\prod_{m=1}^{n_{\iota-1}}\frac{1}{1+\eta_m F_m(T_0)}\sum_{j=n_{\iota-1}+1}^{n_\iota}\eta_j\prod_{m=n_{\iota-1}+1}^{j}\frac{1}{1+\eta_m F_m(T_0)}\\ =&\left(1-S_\iota(T_0)\sum_{j=1}^{n_{\iota-1}}\eta_j\prod_{m=1}^{j}\frac{1}{1+\eta_m F_m(T_0)}\right)\prod_{m=1}^{n_{\iota-1}}(1+\eta_m F_m(T_0)).\end{aligned}$$

□

Proof for Theorem 3.1

Proof. Note that, $n_0 \coloneqq 1, n_1 = 2, n_2 = 3, n_3 = 4$, we have

$$n_\iota - n_{\iota-1} = 1, \iota = 1, 2, 3.$$

Then, based on Proposition 3.1, we have

$$\begin{aligned}&\left(1-S_\iota(T_0)\sum_{j=1}^{n_{\iota-1}}\eta_j\prod_{m=1}^{j}\frac{1}{1+\eta_m F_m(T_0)}\right)\prod_{m=1}^{n_{\iota-1}}(1+\eta_m F_m(T_0))\\ =&\prod_{j=n_{\iota-1}+1}^{n_\iota}\frac{1}{1+\eta_j F_j(T_0)}+S_\iota(T_0)\sum_{j=n_{\iota-1}+1}^{n_\iota}\eta_j\prod_{m=n_{\iota-1}+1}^{j}\frac{1}{1+\eta_m F_m(T_0)}\\ =&\frac{1}{1+\eta_{n_\iota}F_{n_\iota}(T_0)}(1+S_\iota(T_0)\eta_{n_\iota}),\end{aligned}$$

where $f_\iota \coloneqq F_{n_\iota}(T_0)$ can be *uniquely* solved *exactly* in a closed form as

$$f_\iota=\frac{\frac{1}{\eta_{n_\iota}}+S_\iota(T_0)}{\left(1-S_\iota(T_0)\sum_{j=1}^{n_{\iota-1}}\eta_j\prod_{m=1}^{j}\frac{1}{1+\eta_m F_m(T_0)}\right)\prod_{m=1}^{n_{\iota-1}}(1+\eta_m F_m(T_0))}-\frac{1}{\eta_{n_\iota}}.\ \iota=1,2,3. \tag{C1}$$

Based on Proposition 3.1 and the *assumption* (16) for the 1Y $^+$-forward rates, we immediately have

$$\begin{aligned}&\left(1-S_\iota(T_0)\sum_{j=1}^{n_{\iota-1}}\eta_j\prod_{m=1}^{j}\frac{1}{1+\eta_m F_m(T_0)}\right)\prod_{m=1}^{n_{\iota-1}}(1+\eta_m F_m(T_0))\\ =&\prod_{j=n_{\iota-1}+1}^{n_\iota}\frac{1}{1+\eta_j f_\iota}+S_\iota(T_0)\sum_{j=n_{\iota-1}+1}^{n_\iota}\eta_j\prod_{m=n_{\iota-1}+1}^{j}\frac{1}{1+\eta_m f_\iota},\ \iota=4,\ldots,9.\end{aligned} \tag{C2}$$

Note that, approximately $\eta_{n_{\iota-1}-1} = \cdots = \eta_{n_\iota} = \frac{1}{4}$, we can rewrite (C2) as

$$\begin{aligned}&\left(1-S_\iota(T_0)\sum_{j=1}^{n_{\iota-1}}\eta_j\prod_{m=1}^{j}\frac{1}{1+\eta_m F_m(T_0)}\right)\prod_{m=1}^{n_{\iota-1}}(1+\eta_m F_m(T_0))\\ \approx&\prod_{j=n_{\iota-1}+1}^{n_\iota}\frac{1}{1+\frac{1}{4}f_\iota}+S_\iota(T_0)\sum_{j=n_{\iota-1}+1}^{n_\iota}\frac{1}{4}\prod_{m=n_{\iota-1}+1}^{j}\frac{1}{1+\frac{1}{4}f_\iota}\\ =&\frac{1+S_\iota(T_0)\times\frac{1}{4}\sum_{j=n_\iota+1}^{n_\iota}\left(1+\frac{1}{4}f_\iota\right)^{n_\iota-j}}{\left(1+\frac{1}{4}f_\iota\right)^{n_\iota-n_{\iota-1}}}.\end{aligned}$$

By Taylor expansion, we have

$$\left(1+\frac{1}{4}f_\iota\right)^{n_\iota-n_{\iota-1}} \approx 1+(n_\iota-n_{\iota-1})\times\frac{1}{4}f_\iota = 1+f_\iota(T_{n_\iota}-T_{n_{\iota-1}}).$$

$$\frac{1}{4}\sum_{j=n_{\iota-1}+1}^{n_\iota}\left(1+\frac{1}{4}f_\iota\right)^{n_\iota-j} = \frac{1}{4}\sum_{m=1}^{n_\iota-n_{\iota-1}}\left(1+\frac{1}{4}f_\iota\right)^{m-1} = \frac{\left(1+\frac{1}{4}f_\iota\right)^{n_\iota-n_{\iota-1}}-1}{f_\iota}$$

$$\approx \frac{1+(n_\iota-n_{\iota-1})\times\frac{1}{4}f_\iota-1}{f_\iota} = (n_\iota-n_{\iota-1})\times\frac{1}{4} = T_{n_\iota}-T_{n_{\iota-1}}.$$

Hence, we have

$$\left(1-S_\iota(T_0)\sum_{j=1}^{n_{\iota-1}}\eta_j\prod_{m=1}^{j}\frac{1}{1+\eta_m F_m(T_0)}\right)\prod_{m=1}^{n_{\iota-1}}(1+\eta_m F_m(T_0)) \approx \frac{1+S_\iota(T_0)\times(T_{n_\iota}-T_{n_{\iota-1}})}{1+(T_{n_\iota}-T_{n_{\iota-1}})f_\iota},$$

where f_ι can be *uniquely* solved *approximately* in a closed form as

$$f_\iota \approx \frac{\frac{1}{T_{n_\iota}-T_{n_{\iota-1}}}+S_\iota(T_0)}{\left(1-S_\iota(T_0)\sum_{j=1}^{n_{\iota-1}}\eta_j\prod_{m=1}^{j}\frac{1}{1+\eta_m F_m(T_0)}\right)\prod_{m=1}^{n_{\iota-1}}(1+\eta_m F_m(T_0))}-\frac{1}{T_{n_\iota}-T_{n_{\iota-1}}},\ \iota=4,\ldots,9. \tag{C3}$$

By noticing that the mathematical forms of (C1) and (C3) share a lot of similarities, it is possible to combine them into a unified expression (18). Note that, for $\iota=1,2,3$, by definitions (11) and (12),

$$\eta_{n_\iota} = T_{n_\iota}-T_{n_\iota-1} = \zeta_\iota,$$

then, (C1) can be rewritten as the same form as (C3) for $\iota=4,\ldots,9$. "9" □

APPENDIX D: CHANGE OF MEASURE FOR SKELLAM SUMMATION

Theorem D.1. *For a positive constant $\lambda>0$ and any given time point $T>0$, under the equivalent measure $\mathbb{Q}\sim\mathbb{P}$ defined by the Radon–Nikodým derivative*

$$\frac{d\mathbb{Q}}{d\mathbb{P}} = \exp\left((\lambda^++\lambda^--2\lambda)n(T)+\ln\left(\frac{\lambda}{\lambda^+}\right)\sum_{k=0}^{n(T)}N^+(k)+\ln\left(\frac{\lambda}{\lambda^-}\right)\sum_{k=0}^{n(T)}N^-(k)\right), \tag{D1}$$

$\mathbf{D}(T)$ *follows a symmetric Skellam distribution* $\mathrm{SK}(n(T)\lambda, n(T)\lambda)$.

Proof. Obviously, the summation of Skellam random variables still follows a Skellam distribution, that is,

$$\mathbf{D}(t) \coloneqq \sum_{k=0}^{n(t)}D(k) = \sum_{k=0}^{n(t)}(N^+(k)-N^-(k)) = \sum_{k=0}^{n(t)}N^+(k)-\sum_{k=0}^{n(t)}N^-(k),\ t\geq 0,$$

is a Skellam random variable defined by two parameters $(n(t)\lambda^+, n(t)\lambda^-)$. Then, under the natural (data-generating) probability measure $\mathbb{P}$, we have $\mathbf{D}(T)\sim\mathrm{SK}(n(T)\lambda^+, n(T)\lambda^-)$. It is also easy to see that, $\frac{d\mathbb{Q}}{d\mathbb{P}}$ as defined by (D1) is valid to serve as a Radon-Nikodým derivative, because it is a positive random variable and $\mathbb{E}[\frac{d\mathbb{Q}}{d\mathbb{P}}]=1$. Based on the Radon-Nikodým derivative (D1), the MGF of $\mathbf{D}(T)$ under the new measure $\mathbb{Q}$ is given by

$$\begin{aligned}
&\mathbb{E}^{\mathbb{Q}}[e^{v\mathbf{D}(T)}] \\
=\ &\mathbb{E}\left[e^{v\mathbf{D}(T)}\exp\left((\lambda^+ + \lambda^- - 2\lambda)n(T) + \ln\left(\frac{\lambda}{\lambda^+}\right)^{\sum_{k=0}^{n(T)} N^+(k)} + \ln\left(\frac{\lambda}{\lambda^-}\right)^{\sum_{k=0}^{n(T)} N^-(k)}\right)\right] \\
=\ &\exp(\lambda n(T)(e^v - 1) + \lambda n(T)(e^{-v} - 1)),
\end{aligned}$$

which implies that, $\mathbf{D}(T)$ under the new measure $\mathbb{Q}$ still follows a Skellam distribution but with identical parameters $\lambda n(T)$, that is, $\mathbf{D}(T) \sim \mathrm{SK}(n(T)\lambda, n(T)\lambda)$. □

APPENDIX E: PROOF FOR THEOREM 4.1

Proof. It is easy to see that in the assumption (19),[9] the sum of Skellam random variables is still a Skellam random variable, $\mathbf{D}_i(t) \sim \mathrm{SK}\left(n(t)\lambda_i^+, n(t)\lambda_i^-\right)$. Based on Theorem D.1, if the measure $\mathbb{Q}_i$ is defined by the Radon-Nikodým derivative

$$\frac{d\mathbb{Q}_i}{d\mathbb{P}} = \exp\left((\lambda^+ + \lambda^- - 2\lambda_i)n(T_{i-1}) + \ln\left(\frac{\lambda_i}{\lambda^+}\right)^{\sum_{k=0}^{n(T_{i-1})} N_i^+(k)} + \ln\left(\frac{\lambda_i}{\lambda^-}\right)^{\sum_{k=0}^{n(T_{i-1})} N_i^-(k)}\right),$$

then, under the measure $\mathbb{Q}_i$, $\mathbf{D}_i(T_{i-1}) \sim \mathrm{SK}(n(T_{i-1})\lambda_i, n(T_{i-1})\lambda_i)$, so, we have

$$\mathbb{E}^{\mathbb{Q}_i}[F_i(T_{i-1})] = F_i(0) + b\mathbb{E}^{\mathbb{Q}_i}[\mathbf{D}_i(T_{i-1})] = F_i(0).$$

The caplet is a tradable asset, so, its time-t relative price w.r.t. the time-tT_i-bond price $P(t, T_i)$,

$$\frac{\mathrm{Cpl}_i(t)}{P(t, T_i)}, t \in [0, T_i],$$

is a $\mathbb{Q}_i$-martingale, then,

$$\mathbb{E}^{\mathbb{Q}_i}\left[\frac{\mathrm{Cpl}_i(T_i)}{P(T_i, T_i)}\right] = \frac{\mathrm{Cpl}_i(0)}{P(0, T_i)},$$

and we have the time-0 caplet price

$$\begin{aligned}
\mathrm{Cpl}_i(0) &= P(0, T_i)\mathbb{E}^{\mathbb{Q}_i}[\mathrm{Cpl}_i(T_i)] \\
&= \eta_i P(0, T_i)\mathbb{E}^{\mathbb{Q}_i}[(F_i(0) - K + b\mathbf{D}_i(T_{i-1}))^+],
\end{aligned}$$

where

$$\begin{aligned}
&\mathbb{E}^{\mathbb{Q}_i}[(F_i(0) - K + b\mathbf{D}_i(T_{i-1}))^+] \\
=\ &b\sum_{d=-\infty}^{\infty} \Pr\{\mathbf{D}_i(T_{i-1}) = d\}(d - \frac{1}{b}[K - F_i(0)])^+ \\
=\ &b\sum_{d=\lceil\kappa_i\rceil}^{\infty} \Pr\left\{D = d; n(T_{i-1})\lambda_i^+, n(T_{i-1})\lambda_i^-\right\}(d - \kappa_i).
\end{aligned}$$

The PMF of symmetric Skellam distribution is given explicitly by (5), then, we obtain (20). □

[9] In fact, the assumption for the dynamics of $F_i(t)$ is not needed, and only the marginal distribution at the time point T_{i-1} is used here.

APPENDIX F: PROOF FOR SWAP APPROXIMATION

The MGF of a symmetric Skellam random variable $D \sim \mathrm{SK}(\lambda, \lambda)$ is

$$\mathbb{E}[e^{vD}] = \mathbb{E}\left[e^{v(N^+ - N^-)}\right] = \exp(\lambda(e^v - 1) + \lambda(e^{-v} - 1)),$$

then,

$$\begin{aligned}
\mathbb{E}\left[e^{v\sum_{j=1}^{n_\iota} w_j(0)\mathbf{D}_j(T_0)}\right] &= \mathbb{E}\left[e^{v\sum_{k=1}^{n(T_0)}\sum_{j=1}^{n_\iota} w_j(0)D_j(k)}\right] \\
&= \prod_{k=1}^{n(T_0)}\prod_{j=1}^{n_\iota}\exp\left(\lambda_j\left(e^{vw_j(0)} - 1\right) + \lambda_j\left(e^{-vw_j(0)} - 1\right)\right) \\
&\approx \prod_{k=1}^{n(T_0)}\prod_{j=1}^{n_\iota}\exp\left(\lambda_j\left(1 + vw_j(0) + \frac{1}{2}v^2w_j^2(0) - 1\right) + \lambda_j\left(1 - vw_j(0) + \frac{1}{2}v^2w_j^2(0) - 1\right)\right) \\
&= \prod_{k=1}^{n(T_0)}\prod_{j=1}^{n_\iota}\exp\left(\lambda_j w_j^2(0)v^2\right),
\end{aligned}$$

and

$$\begin{aligned}
\mathbb{E}^{\mathbb{S}_\iota}\left[e^{v\sum_{k=1}^{n(T_0)} D^{\mathbb{S}_\iota}(k)}\right] &= \prod_{k=1}^{n(T_0)}\mathbb{E}^{\mathbb{S}_\iota}\left[e^{vD^{\mathbb{S}_\iota}(k)}\right] \\
&= \prod_{k=1}^{n(T_0)}\exp(\lambda^{\mathbb{S}_\iota}(e^v - 1) + \lambda^{\mathbb{S}_\iota}(e^{-v} - 1)) \quad \lambda^{\mathbb{S}_\iota} = \sum_{j=1}^{n_\iota} w_j^2(0)\lambda_j \\
&\approx \prod_{k=1}^{n(T_0)}\prod_{j=1}^{n_\iota}\exp\left(\lambda_j w_j^2(0)\left(1 + v + \frac{1}{2}v^2 - 1\right) + \lambda_j w_j^2(0)\left(1 - v + \frac{1}{2}v^2 - 1\right)\right) \\
&= \prod_{k=1}^{n(T_0)}\prod_{j=1}^{n_\iota}\exp\left(\lambda_j w_j^2(0)v^2\right).
\end{aligned}$$

Therefore, $\sum_{j=1}^{n_\iota} w_j(0)\mathbf{D}_j(T_0)$ and $\sum_{k=1}^{n(T_0)} D^{\mathbb{S}_\iota}(k)$ have approximately the same distribution when $\lambda^{\mathbb{S}_\iota} = \sum_{j=1}^{n_\iota} w_j^2(0)\lambda_j$.

APPENDIX G: PROOF FOR COROLLARY 4.1

The swaption is a tradable asset, so, its time-t relative price with respect to the time-t value of swap annuity $A_\iota(t)$,

$$\frac{\mathrm{PSwpt}_\iota(t)}{A_\iota(t)}, t \in [0, T_0],$$

is a $\mathbb{S}_\iota$-martingale, then,

$$\mathbb{E}^{\mathbb{S}_\iota}\left[\frac{\mathrm{PSwpt}_\iota(T_0)}{A_\iota(T_0)}\right] = \frac{\mathrm{PSwpt}_\iota(0)}{A_\iota(0)},$$

and the time-0 price of the ιth swaption is

$$\mathrm{PSwpt}_\iota(0) = A_{n_\iota}(0)\mathbb{E}^{\mathbb{S}_\iota}\left[\frac{\mathrm{PSwpt}_\iota(T_0)}{A_\iota(T_0)}\right] = A_{n_\iota}(0)\mathbb{E}^{\mathbb{S}_\iota}[(S_\iota(T_0) - K)^+].$$

Based on our distributional assumption (26) for $S_\iota(T_0)$, the remaining proof is the same as the one for Theorem 4.1.